Conformational Energetics of Rhodopsin Modulated by Nonlamellar-Forming Lipids†

Ana Vitória Botelho,‡ Nicholas J. Gibson,§ Robin L. Thurmond,||,⊥ Yin Wang,#,△ and Michael F. Brown*,‡,||

Departments of Biochemistry and Molecular Biophysics, Physics, and Chemistry and Division of Neurobiology, Arizona Research Laboratories, University of Arizona, Tucson, Arizona 85721

Received October 31, 2001; Revised Manuscript Received January 21, 2002

ABSTRACT: Rhodopsin is an important example of a G protein-coupled receptor (GPCR) in which 11-*cis*-retinal is the ligand and acts as an inverse agonist. Photolysis of rhodopsin leads to formation of the activated meta II state from its precursor meta I. Various mechanisms have been proposed to explain how the membrane composition affects the meta I−meta II conformational equilibrium in the visual process. For rod disk membranes and recombinant membranes containing rhodopsin, the lipid properties have been discussed in terms of elastic deformation of the bilayer. Here we have investigated the relation of nonlamellar-forming lipids, such as dioleoylphosphatidylethanolamine (DOPE), together with dioleoylphosphatidylcholine (DOPC), to the photochemistry of membrane-bound rhodopsin. We conducted flash photolysis experiments for bovine rhodopsin recombined with DOPE/DOPC mixtures (0:100 to 75:25) as a function of pH to explore the dependence of the photochemical activity on the monolayer curvature free energy of the membrane. It is well-known that DOPC forms bilayers, whereas DOPE has a propensity to adopt the nonlamellar, reverse hexagonal (H_{II}) phase. In the case of neutral DOPE/DOPC recombinants, calculations of the membrane surface pH confirmed that an increase in DOPE favored the meta II state. Moreover, doubling the PE headgroup content versus the native rod membranes substituted for the polyunsaturated, docosahexaenoic acyl chains (22:6ω3), suggesting rhodopsin function is associated with a balance of forces within the bilayer. The data are interpreted by applying a *flexible surface model*, in which the meta II state is stabilized by lipids tending to form the H_{II} phase, with a negative spontaneous curvature. A simple theory, based on principles of surface chemistry, for coupling the energetics of membrane proteins to material properties of the bilayer lipids is described. For rhodopsin, the free energy balance of the receptor and the lipids is altered by photoisomerization of retinal and involves curvature stress/strain of the membrane (frustration). A new biophysical principle is introduced: matching of the *spontaneous curvature* of the lipid bilayer to the mean curvature of the lipid/water interface adjacent to the protein, which balances the lipid/protein solvation energy. In this manner, the thermodynamic driving force for the meta I−meta II conformational change of rhodopsin is tightly controlled by mixtures of nonlamellar-forming lipids having distinctive material properties.

Among the central questions of biochemistry are the role of the lipid diversity of biomembranes and the relation of lipid properties to protein-mediated cellular functions. According to the fluid-mosaic model (*1*), the lipid bilayer acts as a permeability barrier and is mainly a structural element or matrix for the vectorial organization of membrane proteins (*2*). A key property is a sufficient degree of fluidity of the bilayer, but apart from this aspect the lipids do not play any direct role in the activities of proteins. Moreover, the central paradigm represented by the fluid-mosaic model focuses exclusively on the lamellar phase of membrane lipids. The standard model largely neglects membrane deformation (*3*−*7*) and related dynamical processes (*8*), which correspond to the nonlamellar-forming tendency of many biomembrane lipids (*9*−*15*). Current research indicates that the propensity of membrane lipids to adopt nonlamellar phases may be related to the activities of membrane proteins (*3*, *16*−*19*) and peptides (*20*−*24*). Consequently, the fluid-mosaic model may require modification or possibly replacement by a new biomembrane model.

Recent attention in membrane biochemistry has focused on G protein-coupled receptors (GPCRs),[1] and in this regard rhodopsin is a paramount example (*25*). It is estimated that ≈20% of the genes of the human genome code for membrane proteins, many of which are believed to be GPCRs (*26*). Progress in structural investigations of rhodopsin, e.g.,

† This research was supported by the National Institutes of Health. A.V.B. is the recipient of a scholarship from CAPES, Brasilia, DF, Brazil. R.L.T. was supported by a postdoctoral fellowship from the NIH.

* To whom correspondence should be addressed at the Department of Chemistry, University of Arizona, Tucson, AZ 85721. Phone: (520) 621-2163. Fax: (520) 621-8407. E-mail: mfbrown@u.arizona.edu.

‡ Department of Biochemistry and Molecular Biophysics, University of Arizona.

§ Division of Neurobiology, University of Arizona.

|| Department of Chemistry, University of Arizona.

⊥ Present address: R. W. Johnson Pharmaceutical Research Institute, 3210 Merryfield Road, San Diego, CA 92121.

Department of Physics, University of Arizona.

△ Present address: Department of Biology, University of California at San Diego, La Jolla, CA 92093-0366.

10.1021/bi011995g CCC: $22.00
Published on Web 04/27/2002

employing site-directed spin-label EPR spectroscopy (*27*−*29*), has culminated in elucidation of its X-ray crystal structure (*26*, *30*). Research from this laboratory (*3*, *4*, *18*, *25*, *31*) suggests the bilayer lipid environment is very important in governing the photochemical activity of rhodopsin linked to triggering of the visual process. The effects of membrane lipids on functional parameters of rhodopsin (*3*, *4*, *18*, *25*, *31*−*37*) are comparable to those observed in site-directed mutagenesis studies of the protein in detergent micelles (*38*−*40*). As rhodopsin is a prototype for integral membrane proteins and GPCRs, it is plausible that these findings are generally relevant for structure−function relationships involving biomembranes. Other examples of lipid modulation of protein functions include the activities of Ca^{2+}-ATPase from muscle sarcoplasmic reticulum (*41*), mannosyltransferase II and dolichyl-phosphomannose synthase from liver microsomes (*17*), nicotinic acetylcholine receptor (*42*), Ca^{2+}-activated potassium channel (*43*), and finally the growth of microorganisms (*44*, *45*) as well as eukaryotic cells (*46*). Significant influences of the membrane lipid composition also occur in the case of membrane-embedded peptides (*21*−*24*, *47*, *48*). However, it is mainly for rhodopsin that the effects of bilayer lipids on the conformational energetics of an integral membrane protein have been studied directly in real time, demonstrating a role in protein-mediated function at the molecular level (*3*, *18*, *31*, *33*, *34*, *36*, *37*).

It is known that the lipid composition of the retina includes phosphatidylcholine (PC), phosphatidylethanolamine (PE), and phosphatidylserine (PS), together with highly polyunsaturated fatty acyl groups of the ω3 series, such as docosahexaenoic acid (DHA; 22:6ω3) (*49*, *50*). Studies of animal models have shown that a reduction in DHA is correlated with retinal degeneration, which is accompanied by an increase in retinal PE (*51*). Alteration of retinal DHA is also associated with a perturbation of the photochemistry of rhodopsin in ω3 fatty acid-deficient rats (*52*). One possibility is that the lipid influences are due to specific lipid−rhodopsin interactions (*53*), e.g., in which a single bound PS molecule is released into the bulk lipid phase upon activation of the photoreceptor (*54*). Alternatively, we have proposed that the lipid diversity of membranes is associated with their average or material properties (*4*). Earlier formulations of nonspecific lipid−protein interactions have involved a mattress model, emphasizing hydrophobic matching of the lipids to the protein intramembraneous surface in terms of lipid phase equilibria (*55*, *56*). Recent attention has focused on the possible role of lipid rafts in receptor mechanisms (*57*). Yet in the native retinal rod membranes, the lipids are entirely in the fluid (L_α) phase near physiological temperature (*58*). Here the PE headgroups promote a condensation of the bilayer aqueous interface, whereas the bulky DHA chains favor an increased cross-sectional area, leading to a bending moment of the individual monolayers (*18*). As a result, there is a tendency of the native rod outer segment (ROS) lipids to form nonlamellar, reverse hexagonal (H_{II}) and/or cubic phases (*10*). Following Helfrich (*59*), we have proposed a flexible surface model (*3*, *4*), in which the *spontaneous curvature* of the membrane represents a key aspect. The curvature free energy (g_c) depends on a combination of forces within the headgroup and acyl chain regions of the bilayer and is given by

$$g_c = \kappa(H^L - H_0^L)^2 \quad (1)$$

where κ is the force constant (bending rigidity), H^L is the monolayer curvature of the lipid film, and H_0^L is the natural or spontaneous curvature. A mechanism involving coupling of the elastic area or curvature stress/strain of the planar bilayer lipids (*frustration*) to the chain packing energy at the intramembraneous protein surface yields an energy balance (*3*, *4*) that explains the lipid influences on rhodopsin-mediated functions (*3*, *18*, *33*, *34*, *36*, *37*, *60*). Equivalently, one can consider the lateral pressure profile across the lipid bilayer (*7*, *61*−*63*), or an approach in terms of molecular-level interaction constants can be used (*6*). The concept of elastic stress/strain provides a natural explanation for the combined effects of the phospholipid headgroups and the acyl chain composition on protein-related activities of biomembranes (*4*, *25*).

The research in this paper has further addressed the question of whether such lipid influences are chemically specific (*53*, *54*) or rather originate from nonspecific material properties of the membrane bilayer (*3*, *4*, *25*). A series of lipid substitution experiments were carried out to explore the combined effects of the membrane lipid polar headgroups and acyl chains on rhodopsin function (*3*). Absorption of light leads to 11-*cis* to all-*trans* isomerization of retinal, followed by a conformational change of the protein involving two key intermediate states, meta I and meta II (*25*). The meta II state interacts with a heterotrimeric G protein (transducin), leading to activation of its effector phosphodiesterase and a visual nerve impulse (*64*). Our work has reduced the problem to studies of the meta I−meta II transition of rhodopsin in binary mixtures of dioleoylphosphatidylethanolamine (DOPE) and dioleoylphosphatidylcholine (DOPC). The phospholipids DOPE and DOPC are electrically neutral and have been used for many years to study lipid polymorphism (*11*). Rhodopsin was recombined with various molar ratios of DOPE and DOPC to explore how the energetic parameters of the meta I−meta II transition depend on the membrane lipid composition. Using time-resolved flash photolysis techniques, pH titration curves were obtained for the acid−base metarhodopsin equilibrium on the millisecond time scale following an actinic light pulse. We discovered that PE *headgroups* can compensate for a lack of polyunsaturated *acyl chains*, suggesting that rhodopsin function is associated with a nonspecific balance of forces within the bilayer (*4*). Our results imply that, in recombinants with nonlamellar-forming lipids, the curvature free energy of the membrane film yields a source of work for the meta I−meta II equilibrium. These new findings reveal that material properties of the lipid bilayer (*3*, *4*, *25*) are important in modulating the conformational energetics of integral membrane proteins such as rhodopsin. Several preliminary reports of this research have appeared (*65*, *66*).

[1] Abbreviations: EPR, electron paramagnetic resonance; DHA, docosahexaenoic acid; DOPC, dioleoylphosphatidylcholine; DOPE, dioleoylphosphatidylethanolamine; DTAB, dodecyltrimethylammonium bromide; DTT, dithiothreitol; egg PC, egg yolk phosphatidylcholine; GPCR, G protein-coupled receptor; meta I, metarhodopsin I; meta II, metarhodopsin II; PC, phosphatidylcholine or phosphocholine; PE, phosphatidylethanolamine or phosphoethanolamine; PMT, photomultiplier tube; PS, phosphatidylserine or phosphoserine; ROS, rod outer segment; SPR, surface plasmon resonance.

MATERIALS AND METHODS

Preparation of Native ROS Membranes and DOPE/DOPC Recombinant Membranes. Native ROS membranes were isolated as described (*67*) from frozen bovine retinas (W. L. Lawson Co., Lincoln, NE) and stored at −70 °C under argon. All manipulations were carried out in dim red light (15 W bulb, Kodak Safelight filter no. 1). The A_{280}/A_{500} absorbance ratio was typically 2.4 ± 0.1, as determined spectrophotometrically by solubilizing 100 μL of membranes in 900 μL of a detergent buffer solution comprising 30% (v/v) Ammonyx LO (Stepan Co., Northfield, IL), 100 mM hydroxylamine (Sigma Chemical Co., St. Louis, MO), and 10 mM sodium phosphate, pH 7.0. DOPE and DOPC were obtained from Avanti Polar Lipids (Alabaster, AL) and were used as received. The purification of rhodopsin from ROS membranes (*68*) was performed using a hydroxyapatite column (2.5 × 6.5 cm) (DNA grade Bio-Gel HTP; Bio-Rad Laboratories, Hercules, CA), equilibrated with 100 mM DTAB detergent, 15 mM sodium phosphate, pH 6.8, and 1 mM DTT at 4 °C. A linear gradient of 0.0−0.5 M NaCl was applied with a flow rate of 0.4 mL min^{-1} to elute the rhodopsin. Recombinant membranes were formed by first evaporating mixtures of DOPE/DOPC to a constant weight. Next, the chloroform-free lipids were solubilized in an excess of DTAB. The purified rhodopsin in DTAB corresponding to a total lipid/rhodopsin molar ratio of 100:1 was then added, and the mixture incubated for 45 min at 4 °C. The preparation was dialyzed at 4 °C against 0.5 L mg^{-1} of rhodopsin of 5 mM Hepes buffer containing 1 mM EDTA at pH 6.8, under a constant nitrogen stream, either for 2 days, exchanging the buffer every 4 h (*68*), or for 4 days, exchanging the buffer every 12 h (*3*). Finally, the recombinant membranes were harvested by centrifugation and resuspended in 67 mM sodium phosphate, pH 7.0.

Flash Photolysis Measurements. Flash photolysis data were acquired using a home-built single-beam spectrophotometer, having an optical path length (l) of 5 cm (*3*, *18*, *31*). The instrument was set to monitor changes in light transmission at 478 nm for metarhodopsin I, with a sampling interval of 50 μs and a total acquisition time of 400 ms. The increase in transmittance following flash photolysis was due to formation of meta II from the mixture of rhodopsin and meta I produced by the single actinic light pulse. The fraction of rhodopsin bleached was monitored using a Varian 2290 spectrophotometer as described (*3*). After the UV−visible absorption spectrum of the membranes solubilized in detergent buffer was recorded (cf. above), the samples were fully bleached (six flashes) with a Sunpack AP-52 flash unit fitted with a Schott OG 515 filter (transmission cutoff below 515 nm), which yielded the spectral baseline for the calculations. Measurement of the absorbance change at 500 nm relative to the nonflashed control sample provided the degree of photolysis (≈20−25%). A phototransient was recorded after the first flash, and after numerous flashes were delivered to the sample, or until no change in the output voltage was observed. The repeated flashes yielded a record of the scattered flash lamp afterglow.

For the flash photolysis experiments, the ROS membranes and rhodopsin/DOPE/DOPC recombinants were resuspended in 10 mM sodium phosphate buffer at the desired pH to yield a final rhodopsin concentration of 2.2 μM. Prior to data acquisition, the samples were placed in an ice/water bath and lightly sonicated (Heat Systems-Ultrasonics, Inc., model W375, Plainview, NY) with a 50% duty cycle for 3 min under argon. The influences of the variable light scattering as well as the accuracy of the optical path alignment were compensated by adjusting the electrooptical gain, which is controlled by the voltage across the photomultiplier tube (PMT). In our experiments, the preflash PMT output voltage was set to a constant value of 10 V for all measurements. With this correction, it was found that the sonication procedure did not appreciably change the magnitudes of the flash transients of the membranes (*69*). This also ruled out the possibility of influences of the size or curvature of the membrane preparations, which in the case of the recombinants were ≈4000 Å prior to sonication (*68*). Further control studies showed that the absorbance change (ΔA) due to the meta I−meta II transition was proportional to the fraction of rhodopsin bleached (f) following a single actinic flash. This implied the ratio of ΔA to f was constant under given conditions of temperature and pH. Consequently, the mole fraction of meta II (θ) formed in the meta I−meta II equilibrium was independent of the percentage of rhodopsin bleached in the photolysis experiments.

Reduction and Analysis of Flash Photolysis Data. For the purpose of data analysis, a simple acid−base equilibrium for the meta I−meta II transition was considered, viz., meta I + $\nu H_3O^+ \rightleftharpoons$ meta II, using $\nu = 1$. The stoichiometry of hydronium ions has been previously investigated, yielding values in the range of 0.7−2.0 (*70*−*72*). The molar transmittance at 478 nm following the actinic flash was presumed to be due solely to changes in the concentration of rhodopsin. From the molar absorption coefficient of rhodopsin, $\epsilon_{498}^{rho} = 40\,600\ M^{-1}\ cm^{-1}$ at 498 nm, a value of $\epsilon_{478}^{rho} = 37\,000\ M^{-1}\ cm^{-1}$ at 478 nm was estimated from the experimental absorption spectrum (*3*). The meta I intermediate was assumed to have a molar absorption coefficient of $\epsilon_{478}^{MI} = 44\,000\ M^{-1}\ cm^{-1}$ at 478 nm (*3*). The absorption at 478 nm due to meta II was taken as zero. The postflash change in absorbance at 478 nm, ΔA_{478}, was obtained directly from the voltage difference acquired after the flash and converted to ΔA using the Beer−Lambert law:

$$\Delta A = \log(V_{preflash}/V) - \log(V_{preflash} + \Delta V/V) \quad (2)$$

where V_0 is the incident light voltage and $\Delta V = V_{postflash} - V_{preflash}$. As the preflash voltage was adjusted to a constant value of 10 V (cf. above), the above equation reduced to $\Delta A = 1 - \log(10 + \Delta V/V)$. The mole fraction ($\theta$) of photolyzed rhodopsin in the metarhodopsin II form was obtained (*3*) using $\theta = 0.159 - 2.07\Delta A_{478}/f$. In fitting the pH-dependent flash photolysis data, we used the relation

$$\Delta A_{478} = (1 - \theta)\Delta A_{478}^{MI} + \theta\Delta A_{478}^{MII} \quad (3)$$

where $\Delta A_{478}^{MI} = \Delta\epsilon_{478}^{MI}[rho]_0 l$ and $\Delta A_{478}^{MII} = \Delta\epsilon_{478}^{MII}[rho]_0 l$, i.e., representing the limiting absorbance changes. As noted above, the initial concentration of rhodopsin $[rho]_0/f$ in all experiments was 2.2 μM. The mole fraction (θ) of meta II formed by flash photolysis was given by $\theta = [MII]_{eq}/([MI]_{eq} + [MII]_{eq})$, where the square brackets indicate molar concentrations approximating activities as discussed below. Fitting of the experimental data was accomplished using the

downhill simplex method as implemented in Matlab (The MathWorks, Inc., Natick, MA).

THEORETICAL BACKGROUND

Thermodynamic Model for Coupling of Bilayer Free Energy to Integral Membrane Proteins. Here we provide an expanded description of a novel bilayer-mediated mechanism suggested previously (*3*, *4*). The key idea is that the lipid−protein interactions represent a balance of the elastic stress/strain of the bilayer lipids and the chain packing energy due to the lipid−protein interface (solvation energy of the intramembranous protein surface). First, we note that the case of a membrane is analogous to a solute (the protein) dissolved in a solvent (the lipids). The above system corresponds to an ideal dilute solution of lipids and protein. One can then consider changes of state involving an integral membrane protein, e.g., a G protein-coupled receptor such as rhodopsin. The electrochemical potential for a given state (*i*) is given by

$$\bar{\mu}_i = \mu_i + \mu_i^{\mathrm{el}} \tag{4}$$

where the electrical part is

$$\mu_i^{\mathrm{el}} = z_i F \psi \tag{5}$$

In the above formula z_i is the charge, F is the Faraday constant, and ψ is the electrostatic potential. The nonelectrostatic part, μ_i, of the electrochemical potential (at constant T and P) describes the dependence on concentration and is

$$\mu_i = \mu_i^{\circ} + RT \ln a_i \tag{6}$$

where R is the gas constant, T is the temperature, $a_i = \gamma_i(m_i/m^{\circ})$ is the activity of the ith component, γ_i is the activity coefficient, m_i is the molality, and $m^{\circ} = 1$ m (molal) assuming the Henry's law (°) standard state. (Activities are substituted by relative molar concentrations, indicated by square brackets [ ].) For the equilibrium meta I + $\nu H_3O^+ \rightleftharpoons$ meta II, the standard free energy change is $\Delta G^{\circ} = \mu^{\circ}_{\mathrm{MII}} - \mu^{\circ}_{\mathrm{MI}} - \nu\mu^{\circ}_{\mathrm{H^+}} = -RT \ln K_{\mathrm{eq}}$, where the equilibrium constant is $K_{\mathrm{eq}} = [\mathrm{MII}]_{\mathrm{eq}}/[\mathrm{MI}]_{\mathrm{eq}}[H_3O^+]^{\nu}_{\mathrm{eq}}$, which is *independent of pH*.

In what follows, we further divide the chemical potential into various contributions of interest. First we note that in dealing with pH-dependent equilibria the biochemical standard state is often used. This corresponds to unit activity of all components at the bulk pH at which the sample is buffered, e.g., pH 7.0 (including the hydronium ions), with $\psi = 0$; it is indicated by an additional prime (′). Consequently, the stoichiometry of the hydronium ions does not appear explicitly (*3*), avoiding model-dependent assumptions. The activities (dimensionless) represent the total relative molar concentrations of the various ionized species, e.g., rhodopsin with acidic and basic functional groups. For the meta I−meta II equilibrium, the chemical potentials are $\mu^{\circ\prime}_{\mathrm{MI}} = \mu^{\circ}_{\mathrm{MI}}$, $\mu^{\circ\prime}_{\mathrm{MII}} = \mu^{\circ}_{\mathrm{MII}}$, and $\mu^{\circ\prime}_{\mathrm{H^+}} = \mu^{\circ}_{\mathrm{H^+}} + RT \ln a^{\circ\prime}_{\mathrm{H^+}}$, where $a^{\circ\prime}_{\mathrm{H^+}}$ is the bulk hydronium activity in the biochemical standard state. This gives $\Delta G^{\circ\prime} = \Delta G^{\circ} + \nu RT \ln a^{\circ\prime}_{\mathrm{H^+}} = -RT \ln K'$, in which the apparent equilibrium constant $K' = a_{\mathrm{MII}}/a_{\mathrm{MI}} \equiv [\mathrm{MII}]/[\mathrm{MI}]$ is *pH dependent*.

Let us assume a continuum model for the free energy coupling on the mesoscopic length scale of the bilayer thickness and the embedded protein (*3*, *4*). Such an indirect mechanism for lipid−protein interactions involves the elastic stress/strain of the bilayer lipids, together with the (positive) free energy due to sealing the membrane protein into the bilayer, viz., the protein solvation energy. Consequently, we write for the standard part of the chemical potential that

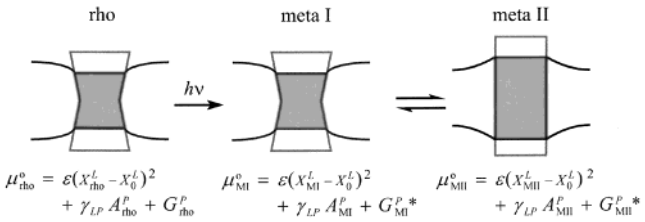

FIGURE 1: New biomembrane model involving coupling of spontaneous curvature of the lipid bilayer to the conformational energetics of an integral membrane protein (*3*, *4*). Rhodopsin is shown as an example of a G protein-coupled receptor (GPCR). The dark-adapted rhodopsin, metarhodopsin I, and metarhodopsin II states (*i*) are depicted, together with their standard chemical potentials μ_i°. Elastic stress/strain of the bilayer is formulated in terms of a generalized modulus ϵ, together with the corresponding geometric variable X_i^{L} and its equilibrium value X_0^{L}. For area stress/strain ϵ is k_a, the area elastic modulus, and $X^{\mathrm{L}} \equiv A^{\mathrm{L}}$ is the lipid/water interfacial area. For curvature stress/strain ϵ is κ, the bending rigidity (splay elastic modulus), and $X_i^{\mathrm{L}} \equiv A_i^{\mathrm{L}}$ is the mean curvature of the opposed monolayers of the bilayer. The lipid/protein interfacial tension is indicated by γ_{LP}, where A_i^{P} is the area of the intramembraneous surface of the protein. Finally, G_i^{P} is the free energy of the protein, where the asterisk indicates that rhodopsin is photoexcited. The increase in the lipid/protein interfacial free energy in the meta II state is balanced by a reduction in curvature elastic stress due to nonlamellar-forming lipids (frustration).

$$\mu_i^{\circ} = \mu_i^{\circ,\mathrm{L}} + \mu_i^{\circ,\mathrm{LP}} + \mu_i^{\circ,\mathrm{P}} \tag{7}$$

Here μ_i° is the standard chemical potential (kJ mol^{-1}) for a given state of the membrane, i.e., corresponding to the Henry's law standard state; $\mu_i^{\circ,\mathrm{L}}$ is the part due to the membrane lipid bilayer; $\mu_i^{\circ,\mathrm{LP}}$ represents the lipid−protein interface; and $\mu_i^{\circ,\mathrm{P}}$ is from the other "internal" protein contributions. According to eq 7, the nonideality of the system is attributed to the lipid component of the membrane and is divided into two parts. The first is due to the lipid bilayer itself ($\mu^{\circ,\mathrm{L}}$) and the second to the lipid−protein interaction ($\mu^{\circ,\mathrm{LP}}$). A further source of nonideality involves the protein−protein interactions, which are assumed to be independent of the lipid composition. The nonideality of the protein in each of its conformational states is described by the corresponding activity coefficient γ_i and gives a constant term to the chemical potential, which is not considered explicitly.

Elastic Deformation of the Membrane Bilayer. Figure 1 illustrates the bilayer-mediated mechanism in schematic fashion for the case of dark-adapted rhodopsin, the metarhodopsin I state, and the activated metarhodopsin II state. The various conformational states are modeled as rigid hydrophobic inclusions having different intramembranous shapes. To put the formulation on a general footing (*4*, *25*), we assume two alternative treatments, either in terms of elastic area deformation of the bilayer surface or, alternatively, in terms of elastic curvature deformation, due to the

spontaneous curvatures of the two opposed monolayer films (*73*).

(i) For the first term in the standard chemical potential, we can write in general that

$$\mu_i^{\circ,\mathrm{L}} = \epsilon(X_i^{\mathrm{L}} - X_0^{\mathrm{L}})^2 \tag{8}$$

i.e., corresponding to a harmonic approximation for the extensive variable. Here, X_i^{L} refers to the appropriate geometric variable describing the free energy of the bilayer lipids in the *i*th state of the membrane, X_0^{L} is the corresponding equilibrium value, and ϵ is the force constant (elastic modulus) that relates the strain $X_i^{\mathrm{L}} - X_0^{\mathrm{L}}$ to the stress. (For large deviations higher order terms are expected in the free energy.) One formulation (*3*, *4*, *55*) involves *area stress/strain* (*frustration*) of the bilayer lipids, due to hydrophobic matching with the protein, giving

$$\mu_i^{\circ,\mathrm{L}} = (\gamma_{\mathrm{LW}}/A_i^{\mathrm{L}})(A_i^{\mathrm{L}} - A_0^{\mathrm{L}})^2 \tag{9a}$$

$$= k_{\mathrm{a}}(A_i^{\mathrm{L}} - A_0^{\mathrm{L}})^2 \tag{9b}$$

In the above formulas $A_i^{\mathrm{L}} - A_0^{\mathrm{L}}$ is the area strain (Å^2), where A_i^{L} is the area per lipid at the aqueous interface, A_0^{L} is the equilibrium lipid area in the absence of protein, γ_{LW} is the interfacial tension of the lipid−protein interface, and k_{a} is the elastic area compressibility modulus (*74*).

Analogously, using differential geometry we can consider the *curvature stress/strain* (*frustration*), in which the geometrical variable is the mean curvature $H = (1/2)(1/R_1 + 1/R_2)$ of the opposed monomolecular films (leaflets) of the bilayer, formulated in terms of a neutral (dividing) plane where the area is constant (*75*). Here $C_1 = 1/R_1$ and $C_2 = 1/R_2$ are the two principal curvatures, allowing for a saddle shape of the hypersurface describing the force balance due to the polar headgroups and the acyl chains of the phospholipid bilayer (*13*, *59*). Displacement of the actual mean curvature H from the equilibrium spontaneous curvature H_0 leads to a curvature elastic stress (free energy). Further generalizing eq 1 leads to (*59*)

$$\mu_i^{\circ,\mathrm{L}} \propto g_{\mathrm{c},i} = \kappa(H_i^{\mathrm{L}} - H_0^{\mathrm{L}})^2 + \bar{\kappa}K \tag{10}$$

where $g_{\mathrm{c},i}$ is the curvature free energy in the *i*th membrane state. In eq 10 H_i^{L} is the mean curvature of the thermodynamic surface corresponding to bending of a given monolayer of the lipid bilayer, H_0^{L} is the corresponding spontaneous curvature, κ is the so-called bending rigidity (the splay elastic modulus), $\bar{\kappa}$ is the modulus of Gaussian (saddle) curvature, and $K = C_1C_2$ is the product of the two principal curvatures. [It is known from studies of colloidal systems that the Gaussian curvature exerts a secondary influence, as described by the Euler characteristic (*13*, *75*).] The curvature elastic properties are related to the moments of the lateral pressure profile of the bilayer, as described by Cantor (*76*). In what follows, we shall only consider the first term in the above expression, eq 10, herein designated as the *curvature free energy*.

(ii) The second term in eq 7 corresponds to the *acyl chain packing energy*, e.g., due to stretching of the lipid acyl chains to match the hydrophobic surface of the protein, i.e., the *protein solvation energy*. It is given by (*4*, *32*)

$$\mu_i^{\circ,\mathrm{LP}} = \gamma_{\mathrm{LP}}A_i^{\mathrm{P}} \tag{11}$$

where γ_{LP} is the interfacial tension of the lipid/protein interface, viz., the work needed for the membrane lipids to solvate the hydrophobic surface of the protein with area A_i^{P} in the *i*th state.

(iii) Finally, the "internal" free energy of the protein inclusion is designated in terms of unspecified other contributions

$$\mu_i^{\circ,\mathrm{P}} = G_i^{\mathrm{P}} \tag{12}$$

in which G_i^{P} is the free energy of the "bare" protein, in the absence of the bilayer lipids.

Flexible Surface Model for Membrane Lipid−Protein Interactions. Let us assume the absorbed photon stimulates photolysis of rhodopsin along its reaction coordinate, yielding a free energy balance due to the elastic stress/strain of the lipid bilayer $\mu_i^{\circ,\mathrm{L}}$, the chain packing energy $\mu_i^{\circ,\mathrm{LP}}$, and the internal protein energy $\mu_i^{\circ,\mathrm{P}}$ for each of the conformations (*i*). A possible molecular correlate is that isomerization of the retinal imparts a strain within the protein, for instance, involving the helix packing (*30*). This could lead to a change in tilt or sliding of the transmembrane helices with respect to the bilayer normal, as suggested by spin-label EPR spectroscopy (*27*−*29*, *77*). We also assume that the local bilayer deformation is described by the curvature free energy, eq 10; similar considerations apply to elastic area deformation. As a result, there is a means of coupling the bilayer curvature stress/strain $\mu_i^{\circ,\mathrm{L}}$ to the protein via the chain packing energy $\mu_i^{\circ,\mathrm{LP}}$ in the various conformational states.

It follows that the standard Gibbs energy change for the meta I−meta II transition can be written as

$$\Delta G^\circ = \Delta\mu^{\circ,\mathrm{L}} + \Delta\mu^{\circ,\mathrm{LP}} + \Delta\mu^{\circ,\mathrm{P}} \tag{13}$$

The electrostatic part, given by eq 5, does not contribute to the standard chemical potential and is described below. Since the nonideality is attributed to the lipids, the $\Delta\mu_i^{\circ,\mathrm{P}}$ term is independent of the membrane composition and provides a constant which does not affect the analysis (vide supra). According to eq 13, there is a *balance* of the free energy contributions from the change in the *curvature stress/strain* $\Delta\mu^{\circ,\mathrm{L}}$ and the *chain packing energy* $\Delta\mu^{\circ,\mathrm{LP}}$. This leads to

$$\Delta G^\circ = \kappa(H_{\mathrm{MII}}^{\mathrm{L}} - H_0^{\mathrm{L}})^2 - \kappa(H_{\mathrm{MI}}^{\mathrm{L}} - H_0^{\mathrm{L}})^2 + \gamma_{\mathrm{LP}}(A_{\mathrm{MII}}^{\mathrm{P}} - A_{\mathrm{MI}}^{\mathrm{P}}) \tag{14}$$

with the appropriate quantity calculus. Assuming the hydrophobic surface of the protein $A_{\mathrm{MII}}^{\mathrm{P}}$ increases in forming meta II (*78*), the contribution from the last term of eq 14 is positive, as it costs free energy to form the lipid/protein interface. Consequently, if the local bilayer curvature $H_{\mathrm{MII}}^{\mathrm{L}}$ changes in the direction of the spontaneous curvature H_0^{L}, then a relief of the curvature stress/strain can occur which is coupled to the mechanical work of the transition. Hence a driving force could result for a protrusion of the protein from the membrane bilayer, as indicated by surface plasmon resonance (SPR) spectroscopy (*78*).

Elastic Energy−Role of Frustration. We next show that the above simple ideas can integrate the results of diverse

studies of lipid influences on the meta I−meta II transition (*3*, *18*, *32*−*35*, *79*, *80*). The curvature free energy is the work needed to deform an individual monolayer film of the bilayer from its spontaneous curvature, H_0^L, to the actual mean curvature H^L, as given by eq 10. It is important to recognize that the free energy contributions from the curvature stress/strain and from the chain packing energy cannot be minimized simultaneously (frustration). In the case of nonlamellar forming lipids, the planar state of the bilayer is under curvature stress/strain and is balanced by the chain packing energy, e.g., due to chain stretching (*11*). Now consider an integral membrane protein, for instance a G protein-coupled receptor such as rhodopsin (cf. Figure 1). According to Figure 1, in the rhodopsin state and the meta I intermediate, the chain packing energy (solvation energy) is less, due to the smaller hydrophobic contact surface of the protein, whereas the elastic (curvature) stress is greater. By contrast, in the meta II state the increased intramembranous area leads to a greater chain packing energy due to hydrophobic matching, whereas the elastic (curvature) stress/strain is less. The reduction of the elastic stress/strain for the opposed monomolecular films of the lipid bilayer, both having a negative spontaneous curvature H_0^L, is due to their curvature H^L toward water (energetically downhill), leading to relief of the curvature frustration. The decrease in elastic free energy compensates for the increased solvation energy of the lipid/protein interface (energetically uphill). Analogous ideas apply for the case of elastic area stress/strain of the bilayer (*3*, *4*).

Contribution of Curvature Free Energy to the Meta I−Meta II Transition. In what follows we are interested in the role of the elastic curvature stress/strain of the lipid bilayer, given by $\mu^{\circ,L} = G_c = ANN_A g_c$. The curvature free energy density is g_c, where A is the area/lipid (≈70 Å^2), N is the number of lipids per rhodopsin, and N_A is Avogadro's number. According to eq 14

$$\ln K_{eq} = -\Delta G^\circ/RT = -ANN_A \Delta g_c/RT - \Delta G_{other}/RT \quad (15)$$

where the "other" free energies in the decomposition, eq 7, are independent of the lipid composition. We consider the curvature free energy per unit area, g_c, and make the assumption that the contributions from the individual components of a lipid mixture are additive (*21*). For a given state (i) of the membrane, cf. eq 10, we have that $g_{c,i} = \kappa(H_i^L - H_0^L)^2$. Our hypothesis is that the curvature free energy change, Δg_c, depends on the mole fraction of nonlamellar-forming lipids in the membrane. In the case of a DOPE/DOPC lipid mixture, the spontaneous curvature is given by $H_0^L = H_0^{DOPE} X_{DOPE}$, where H_0^{DOPE} is the spontaneous curvature of pure DOPE (*81*) and $H_0^{DOPC} \approx 0$. Hence, the change in monolayer curvature free energy for the meta I−meta II transition is

$$\Delta g_c = \kappa(H_{MII}^L - H_0^L)^2 - \kappa(H_{MI}^L - H_0^L)^2 \quad (16a)$$

$$= -2\kappa(H_{MII}^L - H_{MI}^L)H_0^L + \kappa(H_{MII}^{L\,2} - H_{MI}^{L\,2}) \quad (16b)$$

Equations 15 and 16b imply the change in Gibbs free energy ΔG° for the protein conformational change depends linearly on the spontaneous curvature H_0^L of the lipid mixture, e.g., comprising DOPE and DOPC. Differentiating with respect to X_{DOPE} gives the result that

$$\frac{\partial \ln K_{eq}}{\partial X_{DOPE}} = \left(\frac{2\kappa AN}{k_B T}\right)(H_{MII}^L - H_{MI}^L)H_0^{DOPE} \quad (17)$$

where $k_B = R/N_A$ is the Boltzmann constant, and H_{MII}^L and H_{MI}^L are the mean curvatures of the meta II and meta I states, respectively. According to eq 17, the Gibbs free energy change depends linearly on the mole fraction X_{DOPE} in the recombinant membranes.

Poisson−Boltzmann Treatment of Bulk versus Surface pH. As mentioned above, one also needs to consider the electrostatic contribution to the free energy; cf. eq 5. In the present example, the surface potential (ψ_0) originates from the charge of rhodopsin, which depends on the pH, as well as anionic lipids such as PS in the ROS membranes. Here we need to separate the "direct" electrostatic influences on the bilayer elasticity from the "indirect" effects of the ionic composition of the electrical double layer (*82*, *83*). Due to the surface charge density, there are two possible contributions that can oppose or reinforce each other: (i) The surface charge can alter the concentration of hydronium ions, H_3O^+, in the electrical double layer, thereby affecting the meta I−meta II equilibrium due to the proton uptake. Clearly the negative charge due to PS will increase the surface concentration of H_3O^+ ions, favoring meta II (*3*, *84*). (ii) The surface charge (independent of charge sign, viz., ±) is expected to lead to a decrease in the spontaneous curvature H_0^L, favoring the planar state ($H_0^L = 0$). Given a flexible surface model, this will oppose the effect of PS on the local H_3O^+ concentration and favors the meta I state.

The above treatment implies that the electrostatic contribution to the Gibbs function can be separated from the nonelectrostatic part in terms of its effect on the H_3O^+ concentration at the membrane surface. The influence of the membrane surface potential ψ_0 on the distribution of hydronium ions is treated by equating their electrochemical potential, $\bar{\mu}$, as given by eqs 4 and 5, at the membrane surface ($\psi = \psi_0$) and in the bulk solution ($\psi = 0$). This yields $[H_3O^+]_{local} = [H_3O^+]_{bulk}\, e^{-zF\psi_0/RT}$, where $z = 1$ is the protonic charge. It follows that the local and the bulk pH values are related by (*85*)

$$pH_{local} = pH_{bulk} + zF\psi_0/2.303RT \quad (18)$$

The surface potential ψ_0 is calculated by applying the Poisson−Boltzmann equation, which for a planar surface corresponds to the Gouy−Chapman model (*82*); this is further described below.

Moreover, for a titratable membrane surface, one must distinguish between the *apparent* acid ionization constant (pK_{app}) and the *intrinsic* acid ionization constant (pK_{int}) (*86*). The apparent pK_a is related to the intrinsic pK_a by (*82*, *85*)

$$pK_{app} = pK_{int} + \nu zF\psi_0/2.303RT \quad (19)$$

Then, the dependence of the mole fraction of meta II (θ) on the bulk solution pH is given by

$$\theta = 1/(1 + 10^{\nu pH_{bulk} - pK_{app}}) \quad (20)$$

Here $K_{app} = 1/K_{eq}^{app}$ and $K_{eq}^{app} = [MII]/[MI][H_3O^+]_{bulk}^{\nu} = \exp(-\Delta\bar{G}/RT)$, where $\Delta\bar{G} = \Delta G^\circ + \nu zF\psi_0$, which follows

from eq 4. Because the apparent pK_a depends on the membrane surface potential ψ_0, which itself is pH dependent, a plot of θ as a function of bulk pH is broadened compared to a simple two-state equilibrium. Alternatively, the meta II fraction can be recast in terms of the *local* pH and the intrinsic pK_a,

$$\theta = 1/(1 + 10^{\nu pH_{local} - pK_{int}}) \quad (21)$$

which gives a Henderson−Hasselbalch titration curve as a function of the local pH, where $K_{int} = 1/K_{eq}^{int}$ and $K_{eq}^{int} = [MII]/[MI][H_3O^+]_{local}^{\nu} = \exp(-\Delta G°/RT)$. It follows that one can plot the titration curves versus the bulk pH to obtain pK_{app}, according to eq 20, or versus the local pH using eq 21 to obtain pK_{int} (*82*, *85*). In either case the pK_a is the value of the pH where $\theta = {}^1/_2$. As the thermodynamic state functions depend on the local pH, we have previously reported their values assuming the biochemical standard state (*3*).

Next, the Gouy−Chapman equation is used to relate the membrane surface potential ψ_0 to the membrane surface charge density, given by

$$\sigma = (C^{1/2}/A) \sinh (zF\psi_0/2RT) \quad (22)$$

where C is the molar salt concentration due to the sodium phosphate buffer, $z = 1$ is the salt valence, and $A = 136.6$ $M^{1/2}$ Å^2 (*86*). In addition, the total surface charge density per rhodopsin unit cell can be directly calculated using $\sigma = \Sigma\sigma_{basic}^{(i)} - \Sigma\sigma_{acidic}^{(j)} - \sigma_{PS}$. The charge density contributions from the basic amino acid residues are given by

$$\sigma_{basic}^{(i)} = N/(1 + 10^{pH_{local} - pK_i}) \quad (23)$$

in which N is the total surface density of ionizable groups, assuming a surface area of 4000 Å^2 per rhodopsin unit cell, and pK_i is the acid ionization constant of the ith titratable group. Similarly, for the acidic amino acid residues of rhodopsin, the charge density is

$$\sigma_{acidic}^{(j)} = N[1 - 1/(1 + 10^{pH_{local} - pK_j})] \quad (24)$$

where pK_j is the jth acid ionization constant. In the case of the ROS membranes, the contribution of PS to the charge density is computed from (*72*, *86*)

$$\sigma_{PS} = N/[1 + ([H_3O^+]/K_H + [Na^+]/K_{salt})\, e^{-F\psi_0/RT}] \quad (25)$$

Here the K_H is the dissociation constant for H_3O^+, K_{salt} is the dissociation constant for Na^+ buffer binding to PS (1/0.7 M), $[H_3O^+]$ and $[Na^+]$ are the bulk concentrations in the phosphate buffer, and the intrinsic pK_a value for the PS carboxyl group is 3.6 (*72*, *85*). By iteratively solving the above system of nonlinear equations, the charge density can be eliminated and the surface potential ψ_0 used to calculate the local membrane pH using eq 18. Comparison of the data at the same local pH values then allows one to separate the electrostatic contribution of the H_3O^+ ions in the electrical double layer from the intrinsic or nonelectrostatic part of the bilayer free energy.

RESULTS

The Photochemistry of Rhodopsin Is Perturbed in Recombinants with DOPC. Representative flash photolysis results for rhodopsin/DOPC (1:100) recombinant membranes and the native ROS membranes at $T = 28$ °C and different pH values are depicted in Figure 2. The increase of the photomultiplier tube (PMT) output voltage at 478 nm following the actinic flash monitors the transient loss of absorbance due to meta I ($\lambda_{max} = 478$ nm) on the millisecond time scale and the concomitant production of meta II ($\lambda_{max} = 380$ nm). Earlier work (*3*, *18*) has established that the meta I−meta II transition is essentially unaffected by the transbilayer asymmetry of the lipid and protein distributions of the native ROS membranes (*25*), allowing direct comparison to the data for the recombinant membranes having a random orientation. Parts a and b of Figure 2 contrast the results at $T = 28$ °C for rhodopsin in the ROS membranes and DOPC recombinant membranes at pH 7.0 and 5.0, respectively. For the DOPC recombinant at pH 7.0, part a, a substantially diminished phototransient amplitude is observed, whereas nearly the maximum amount of meta II is formed in the native ROS membranes. The greater noise in the rhodopsin/DOPC recombinant membrane sample is due to increased light scattering, requiring a larger electrooptical gain of the PMT (cf. Materials and Methods). In addition, a larger initial artifact due to the flash lamp afterglow is evident for the more strongly scattering samples due to the higher PMT gain. The phototransients in part a indicate that the meta I and meta II states depend on the membrane environment and that

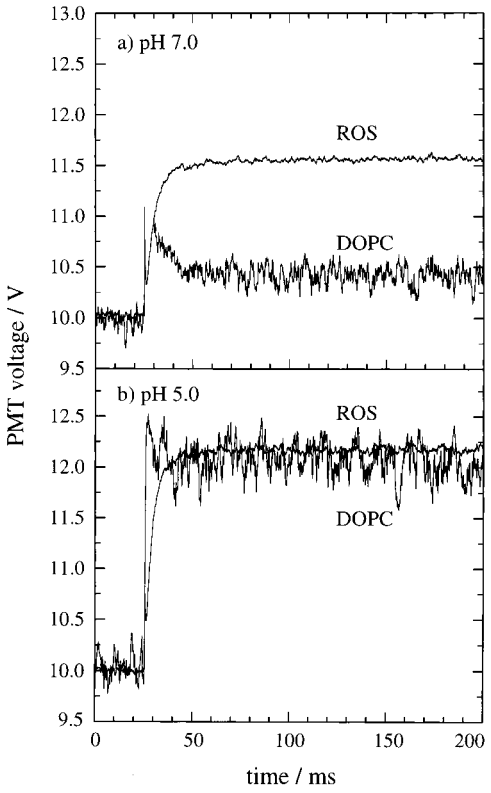

FIGURE 2: Photomultiplier tube (PMT) voltage at $\lambda = 478$ nm following a single actinic flash for rhodopsin/DOPC recombinant membranes compared to native ROS membranes at $T = 28$ °C. In part a, the PMT voltage reveals a smaller change at pH 7.0 for the rhodopsin/DOPC recombinant compared to the native ROS membranes. (The initial overshoot for the DOPC recombinant is a flash artifact due to light scattering.) By contrast, part b shows that the PMT increase at pH 5.0 is similar in both cases. The differences in photochemical behavior reveal the sensitivity of the meta I−meta II equilibrium to the membrane environment.

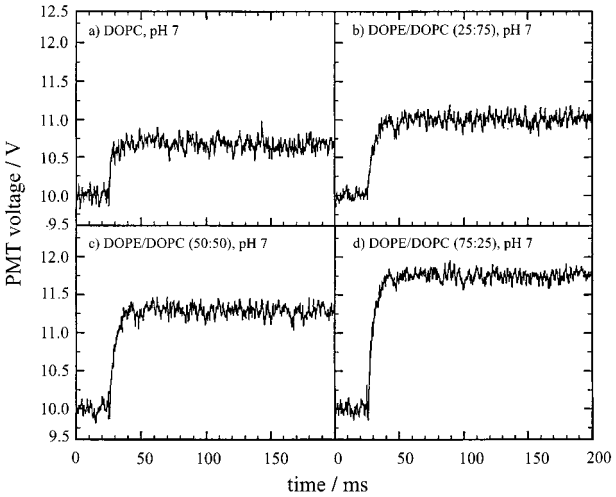

FIGURE 3: Flash photolysis transients acquired at 478 nm, showing the influence of DOPE on the photochemical activity of rhodopsin at $T = 28$ °C and pH 7.0. (a−d) Molar ratios of DOPE/DOPC per rhodopsin of 0:100, 25:75, 50:50, and 75:25, respectively. At *neutral pH* the magnitude of the final PMT voltage is progressively greater as the mole fraction of DOPE increases. The final voltage for the DOPE/DOPC (75:25) recombinant is approximately the same as for the native ROS membranes.

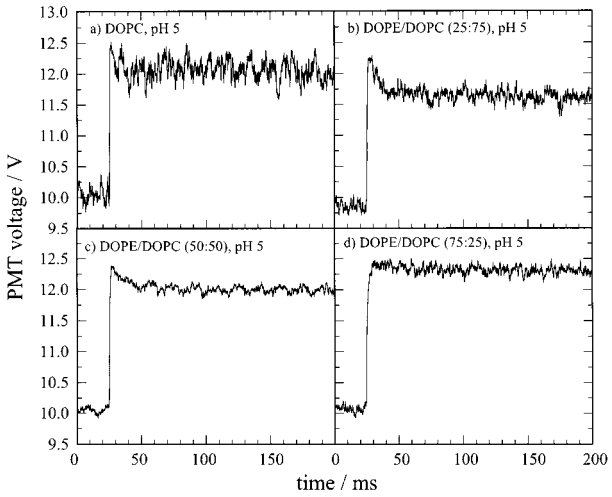

FIGURE 4: Flash photolysis transients obtained at $\lambda = 478$ nm for rhodopsin in DOPE/DOPC recombinant membranes at $T = 28$ °C and pH 5.0. (a−d) Molar ratios of DOPE/DOPC per rhodopsin of 0:100, 25:75, 50:50, and 75:25, respectively. At *acidic pH* the magnitude of the photomultiplier voltage is only slightly affected by the membrane lipid composition, so that the final PMT voltage is similar to that of the native ROS membranes.

lipid modulation of the transition occurs. By contrast, part b reveals that at pH 5.0 the phototransient amplitudes of rhodopsin in the DOPC recombinant as well as the native ROS membranes are essentially equal, with nearly the full amount of meta II formed in each case. These data clearly show that the differences for rhodopsin in the DOPC recombinant and in the ROS membranes are due to a thermodynamically reversible modulation of the meta I−meta II equilibrium caused by the membrane lipid environment (*69*). According to Le Châtelier's principle, the increased $[H_3O^+]$ at acidic pH values drives the equilibrium essentially to completion in both cases.

The Meta I−Meta II Transition Depends on the Mole Fraction of DOPE in Recombinant Membranes. The rhodopsin/DOPE/DOPC membranes were designed to have the following molar lipid ratios per rhodopsin: 0:100, 25:75, 50:50, and 75:25. Flash photolysis signals for rhodopsin in the series of membrane recombinants having different DOPE/DOPC molar ratios at pH 7.0 are depicted in Figure 3. As can be seen, the most striking difference among the recombinant membrane preparations involves the amplitudes of the phototransients. Parts a−d of Figure 3 reveal that a greater mole fraction of DOPE leads to a progressive increase of the PMT voltage change (ΔV) at pH 7.0. The diminished phototransient magnitudes of the recombinants are not due to the higher lipid/protein ratio compared to the ROS membranes (*87*), as studies of egg PC recombinants show only a ≈10% reduction in the mole fraction of meta II on increasing from 75 to 100 lipids/rhodopsin (*69*). Hence, increasing the mole fraction of phosphoethanolamine headgroups in the recombinant membranes leads to a greater production of the activated meta II state at neutral pH. By contrast, Figure 4 shows that at pH 5.0 nearly the same photomultiplier output signal is seen for the identical series of DOPE/DOPC recombinant membranes. Essentially the full amount of meta II is produced at acidic pH values; i.e., the reaction is driven to completion in each case, with little difference among the DOPE/DOPC recombinants. In consequence, the effect of phosphoethanolamine headgroups is an increase of the pK_a of the acid−base metarhodopsin equilibrium for bilayers having only monounsaturated oleoyl (18:1) chains at $T = 28$ °C, close to physiological temperature.

It is worth noting that, on account of the relatively long flash duration of ≈5 μs, the rhodopsin photointermediates can in principle absorb a second photon to yield either rhodopsin (11-*cis* retinylidene chromophore) or isorhodopsin (9-*cis* chromophore). Differences in secondary photolysis events could potentially cause variations in the yield of meta II, possibly explaining the differences in the phototransient magnitudes. However, the fraction of rhodopsin bleached (f) by the single actinic flash was similar in all experiments (20−25%), as measured by the loss of the absorbance peak at 500 nm in the presence of hydroxylamine, which traps the photolysis intermediates as opsin + retinal oxime (*88*). Consequently, the total amount of meta I and meta II is approximately the same in all cases. Conservation of mass then indicates that the differences in phototransient magnitudes reflect the ratio of meta I and meta II coexisting upon photolysis.

The pH dependence of the meta I−meta II equilibrium was further investigated for the DOPE/DOPC recombinants and native ROS membranes by conducting flash photolysis experiments over an extended pH range. The analysis and reduction of the flash photolysis data are illustrated in Figure 5, which shows the effects of progressively increasing the mole fraction of DOPE in the binary lipid recombinants with DOPC. The observed photomultiplier output voltage change (ΔV) was converted to the absorbance change (ΔA) and to the mole fraction of metarhodopsin II (θ) produced after the flash. As an initial approximation, simultaneous fits of the experimental data to a simple titration equilibrium were performed according to eqs 3 and 20 using Matlab, either neglecting the absorbance change at 478 nm due to meta I (dotted lines) or assuming a positive value (dashed lines)

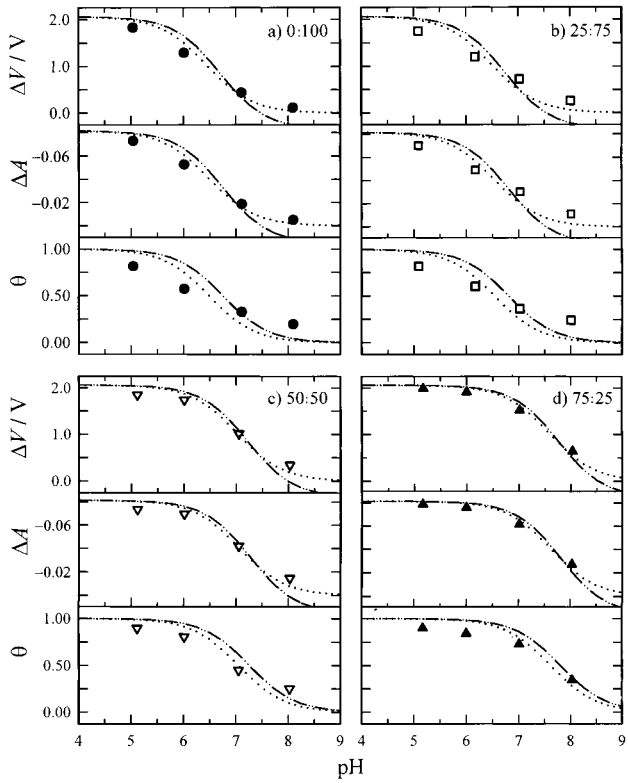

FIGURE 5: Illustration of analysis and reduction of flash photolysis results. Data (averaged) were acquired at $\lambda = 478$ nm for rhodopsin in recombinants with binary DOPE/DOPC mixtures as a function of pH at $T = 28$ °C. The postflash photomultiplier voltage (ΔV), absorbance change (ΔA), and the mole fraction of meta II (θ) are shown. (a−d) Recombinants having DOPE/DOPC molar ratios per rhodopsin of 0:100, 25:75, 50:50, and 75:25, respectively. The fits assume the contribution of meta I to the absorbance change is either positive (-••-) or negligible (•••) with a bleached fraction of $f \approx 20\%$. A progressive shift of the apparent pK_a value is evident as the mole fraction of PE headgroups is increased to approximately double that of the native ROS membranes.

(*3*). In Figure 5, parts a−d, the values are plotted as a function of pH for rhodopsin in the series of DOPE/DOPC recombinants. The results indicate that the fraction of the meta II state increases with a reduction of the bulk pH of the sample medium. Assuming a two-state, acid−base titration equilibrium, *apparent* pK_a values of 6.6 ± 0.3, 6.8 ± 0.3, 7.3 ± 0.2, and 7.8 ± 0.1 are obtained for rhodopsin in the recombinant membranes with increasing DOPE/DOPC molar ratios ranging from 0:100 to 75:25 at $T = 28$ °C, respectively. A broadening of the titration curves is also evident, as further discussed below.

Most remarkably, these data show that, by essentially doubling the native mole fraction to ≈75%, the PE *headgroups* can compensate for the DHA *chains* of the native ROS membranes to yield full photochemical activity in the binary lipid membrane recombinants. The experimental findings are summarized in Figure 6, which includes additional data obtained for the meta I−meta II transition of rhodopsin in the series of DOPE/DOPC recombinants. In parts a−d, the absorbance changes are depicted, together with reference Henderson−Hasselbalch pH titration curves for rhodopsin in the egg PC recombinant membranes and the native ROS membranes. (Note that the pH titration behavior of an amphoteric membrane surface is more complex; cf. Theoretical Background.) The progressive shift of the

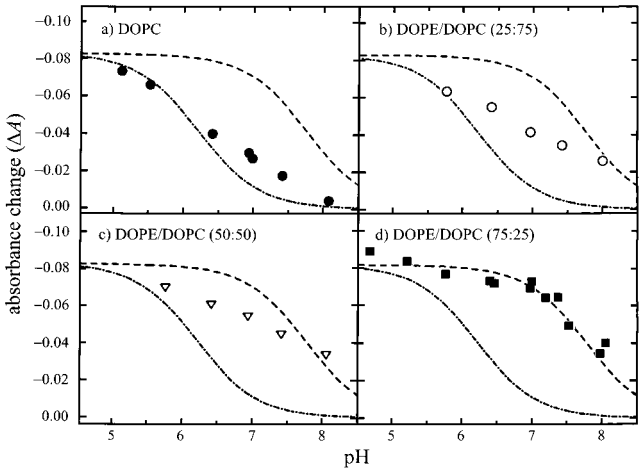

FIGURE 6: Summary of absorption changes due to meta I−meta II transition of rhodopsin in DOPE/DOPC recombinants at $T = 28$ °C. Additional flash photolysis data are plotted as a function of the bulk solution pH, yielding titration curves for the meta I−meta II equilibrium on the millisecond time scale. (a−d) Molar ratios per rhodopsin of 0:100, 25:75, 50:50, and 75:25, respectively. Reference data are included for the native ROS membranes (- - -) and rhodopsin/egg PC (1:100) recombinant membranes (-•-) (*3*). As the DOPE/DOPC ratio is increased, a progressive shift of the pH titration curve to the right is seen; i.e., more meta II is produced. The DOPE/DOPC (75:25) recombinant, part d, has approximately double the native mole fraction of PE and resembles the behavior of the native ROS membranes.

Table 1: Apparent Standard Gibbs Energy Changes for the Meta I−Meta II Equilibrium of Rhodopsin in DOPE/DOPC Recombinant Membranes at 28 °C

	fraction of meta II (θ)		$\Delta G^{\circ\prime}$/kJ mol^{-1} [a]	
sample	pH 5[b]	pH 7[b]	pH 5[b]	pH 7[b]
DOPE/DOPC[c]				
0:100	0.91 ± 0.01	0.35 ± 0.03	−5.9 ± 0.4	+1.5 ± 0.3
25:75	0.88 ± 0.01	0.47 ± 0.02	−5.0 ± 0.4	+0.3 ± 0.2
50:50	0.92 ± 0.01	0.59 ± 0.02	−6.1 ± 0.5	−0.9 ± 0.2
75:25	0.97 ± 0.01	0.79 ± 0.01	−8.9 ± 0.4	−3.4 ± 0.2
ROS membranes	0.95 ± 0.01	0.85 ± 0.03	−7.6 ± 0.2	−4.3 ± 0.6

[a] The biochemical standard state is assumed, i.e., corresponding to the bulk pH. [b] Bulk pH values of 5.08 ± 0.07 and 7.05 ± 0.04 (mean ± S.D.) were measured before the actinic flash. Calculations utilized the percentage of rhodopsin bleached (*f*) as determined for the individual samples. [c] The lipid/rhodopsin molar ratio was 100:1.

apparent pK_a for the meta I−meta II transition to higher values is striking. These results demonstrate that the energetics of the conformational transition of rhodopsin from meta I to meta II differ markedly in these recombinant membranes. Full nativelike photochemical function of rhodopsin is found only in the DOPE/DOPC (75:25) recombinant, suggesting that there is an optimized structure favoring meta II in the native ROS membranes. From the fits of the data to a simple acid−base equilibrium, the apparent standard Gibbs energy changes $\Delta G^{\circ\prime}$ for the meta I−meta II transition of rhodopsin in the series of DOPE/DOPC recombinants were calculated using $\Delta G^{\circ\prime} = -RT \ln K'(\text{pH},T)$, where $K' = \theta/(1 - \theta)$. Table 1 summarizes the thermodynamic results for pH 5 and 7 at $T = 28$ °C, respectively. Comparing the values of $\Delta G^{\circ\prime}$, it is evident that the free energy change becomes more negative as the mole ratio of DOPE to DOPC increases, approaching the value for the native ROS membranes. Thus increasing

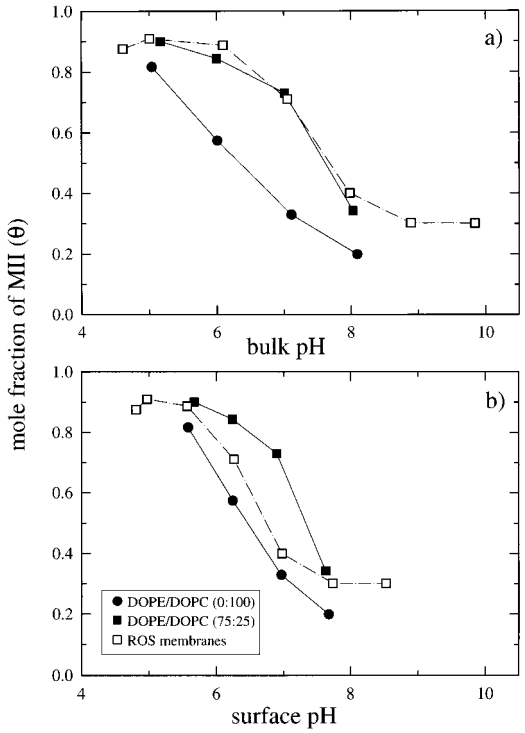

FIGURE 7: Comparison of influences of bulk solution pH and membrane surface pH on the meta I−meta II transition of rhodopsin in DOPE/DOPC recombinant membranes and native ROS membranes. The mole fraction of meta II (θ) produced by a single actinic flash (cf. Figure 5) is plotted for recombinants containing DOPE/DOPC molar ratios per rhodopsin of 0:100 (●) and 75:25 (■) in comparison to the ROS membranes (□). (a) Mole fraction of meta II as a function of the bulk solution pH determined potentiometrically. (b) Mole fraction of meta II versus membrane surface pH calculated using the Gouy−Chapman theory. A symmetric transbilayer distribution of the lipids and rhodopsin is assumed. (For the ROS membranes little difference is seen for symmetric and asymmetric distributions; not shown.) Note that the *intrinsic* pK_a value for the DOPE/DOPC (75:25) recombinant (7.5 ± 0.01) is greater than for the native ROS membranes (7.0 ± 0.2); i.e., more meta II is produced at the same local pH.

DOPC favors the meta I form of photolyzed rhodopsin, whereas increasing the DOPE content favors meta II.

Electrostatic Treatment of the Meta I−Meta II Transition and the Role of Bilayer Deformation. In addition, the membrane surface charge can influence the meta I−meta II equilibrium of rhodopsin. The membrane surface potential arises from the amphoteric rhodopsin molecules, as well as the presence of PS headgroups in the ROS membranes, and governs the accumulation of protons and other cations within the diffuse electrical double layer adjacent to the membrane surface (*82*). By keeping the $[H_3O^+]$ relatively high in the electrical double layer, the presence of PS headgroups can help to drive the meta I−meta II equilibrium to the right (Le Châtelier's principle). Here we have applied a charged-delocalized picture to study the effect of the membrane electrostatics, involving application of the Gouy−Chapman model for treatment of the thermodynamic properties of charged membrane surfaces (*82*, *86*).

Figure 7 illustrates how the membrane environment of rhodopsin influences the meta I−meta II transition, when account is taken of the local hydronium ion concentration at the bilayer surface. An iterative simplex fit of the charge density σ calculated using the Gouy−Chapman model, eq 22, and the charge density calculated directly using eqs 23−25 was performed using Matlab. For the native ROS membranes, similar results are obtained for either an asymmetric or a symmetric transbilayer distribution of the lipids and rhodopsin, consistent with equilibration of the charged lipid pool with the protein in both cases (*83*). In part a, the flash photolysis data are expressed as the mole fraction of meta II versus the *bulk* solution pH, according to eq 20. As can be seen, the titration curves are broadened compared to a simple two-state acid−base equilibrium. The pH titration curve for rhodopsin in the DOPC recombinant is shifted to lower apparent pK_a values compared to the ROS membranes, whereas the 75% DOPE recombinant closely parallels the native behavior (vide supra). On the other hand, part b shows that if the data are plotted against the *local* pH according to eq 21, there is a substantial modification of the meta II fraction compared to the *bulk* pH. A narrowing of the titration curves is evident, approaching the behavior expected for a simple acid−base equilibrium. For the native ROS membranes, the pK_a value is decreased from an apparent value of 8.0 ± 0.2 to an intrinsic value of 7.0 ± 0.2, a difference of about 1.0 unit. The calculated surface pH gives an intrinsic pK_a value approximately equal to that for titration of a histidine residue. Note that the intrinsic pK_a value of 7.5 ± 0.01 is higher in the DOPE/DOPC (75:25) recombinant in part b of Figure 7. Interestingly, it is now the ROS membranes that are less active in producing meta II. Thus the *intrinsic* bilayer properties of the native ROS membranes are actually *less favorable* to forming meta II than in the case of the neutral DOPE/DOPC recombinants.

Dependence of the Meta I−Meta II Free Energy Change on the Lipid Spontaneous Curvature Supports a Flexible Surface Model. The present application is simplified by the fact that neutral lipid mixtures comprising DOPE and DOPC are mainly considered, allowing comparison at equivalent bulk pH values (cf. Figure 7). In Figure 8 the applicability of the flexible surface model to the meta I−meta II transition of rhodopsin is tested in greater detail. Here we have considered the relation of the apparent standard Gibbs energy change $\Delta G^{\circ\prime} = -RT \ln K'$ to the mole fraction of DOPE and to the spontaneous curvature H_0 of the reverse hexagonal phase cylinders of the DOPE/DOPC lipid mixtures in the absence of protein. (The results use the apparent equilibrium constant K' in place of K_{eq}, which gives a constant offset.) Part a shows a plot of $\ln K'$ against the DOPE mole fraction in the recombinant membrane lipid mixtures at pH 7.0. According to Theoretical Background, eq 17, a linear dependence of $\ln K'$ on X_{DOPE} is expected. Moreover, part b shows that $\ln K'$ varies linearly with the experimental value of the inverse of the radius R_w of the aqueous core, as determined for the corresponding H_{II} phase lipids in the presence of *n*-alkanes (related to the spontaneous curvature H_0^L) (*21*, *81*), consistent with eq 16b. Hence, we conclude that the flexible surface model, involving curvature frustration as a mechanism for coupling the free energy of the bilayer lipids to rhodopsin, provides a satisfactory explanation of the experimental data.

DISCUSSION

Currently, the most thoroughly understood G protein-coupled receptor is rhodopsin (*26*, *30*, *39*, *89*, *90*), which

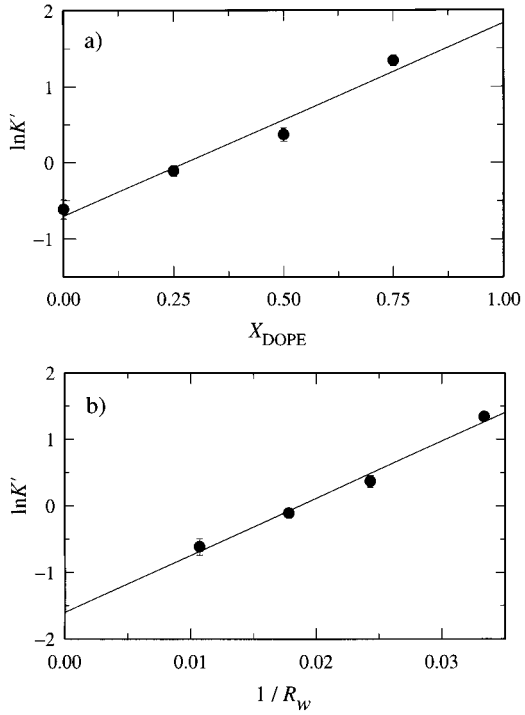

FIGURE 8: Test of the hypothesis that the meta I−meta II equilibrium of rhodopsin is governed by the curvature free energy of neutral membrane lipid mixtures. Semilogarithmic plots of the apparent equilibrium constant K' for the meta I−meta II transition at pH 7.0 and $T = 28$ °C are shown (cf. Figure 5), where $\Delta G^{\circ\prime} = -RT \ln K'$. (a) Plot of $\ln K'$ against the mole fraction of DOPE, X_{DOPE}, in the rhodopsin/DOPE/DOPC recombinant membranes. (b) Graph of $\ln K'$ versus effective spontaneous curvature of the DOPE/DOPC mixtures, defined as the inverse of the water core radius R_w of H_{II} phase cylinders in the presence of excess *n*-alkanes (*21*, *81*). A nearly linear dependence is observed in either case, suggesting that the spontaneous curvature of the membrane lipid mixtures governs the conformational energetics of photolyzed rhodopsin (cf. text).

comprises seven transmembrane helices (*30*, *91*) and is strongly affected by lipid−protein interactions (*3*, *4*, *18*, *25*, *32*−*37*, *60*, *79*, *80*). Present knowledge indicates that the activated form of the protein is meta II, in which the retinal Schiff base of Lys^{296} is deprotonated, breaking the salt bridge to its counterion, the carboxylate group of Glu^{113}. Subsequent proton uptake involves the protonation of a histidine residue (*92*) or possibly Glu^{134} of rhodopsin (*72*, *90*). Previous studies of lipid substitutions on rhodopsin function have shown that the meta I−meta II equilibrium can be modulated by the following: the acyl chain length (bilayer thickness) (*4*, *31*), unsaturation of the acyl chains (*18*, *33*), cholesterol (*60*), the lipid headgroup size (interfacial area) (*3*, *18*), and the headgroup charge of the lipids (*3*, *84*, *93*). An interesting aspect is that, compared to the native ROS membranes, all of the various factors yield a similar result. That is, the apparent pK_a for the meta I−meta II equilibrium is shifted to lower values; i.e., the pH titration curve is displaced to the left. This implies there must be a common change occurring in the membrane, which directly affects the protein. Hence the membrane bilayer may provide a source of work for conformational changes of integral membrane proteins, such as rhodopsin, which can be regarded as a nanoscale engine or a molecular force transducer.

One possibility is that chemically specific properties of the lipids (*54*) are required for the maximum, nativelike photochemical function of rhodopsin. Although specific lipid−protein interactions (*53*, *54*) involving release of a bound PS molecule upon activation of rhodopsin (*54*) may be important, they do not account for the influences of PS and PE headgroups on the meta I−meta II transition (*3*, *84*), which involve substantially larger numbers of lipid molecules. On the other hand, nonspecific material properties of the entire assembly may be involved (*4*). In earlier work (*3*) we have concluded that the meta II state is favored by properties of mixtures of the lipids in the membrane. The combined effects of the lipid polar headgroups and nonpolar acyl chains point to the role of *material properties* (*3*, *4*) in modulating the conformational energetics of rhodopsin (*3*, *18*). The above picture is consistent with the phospholipid composition of the native ROS membranes, which comprises nearly 50% docosahexaenoic acid (DHA) acyl chains (*50*). Electrically neutral DHA chains, in combination with PE, are known to favor a "wedge shape" on average for the membrane lipids, promoting a negative monolayer curvature (*94*), and are important for optimal function of rhodopsin under physiological conditions (*18*). The influences of the lipid headgroups and acyl chains (*3*) are consistent with *curvature elastic stress* as a basis for the influences of neutral lipids on rhodopsin function. Such a mechanism involving coupling of the lipid membrane to the conformational energetics of rhodopsin is a molecular realization (*3*, *18*) of the homeostasis of membrane elastic stress (*12*, *44*, *95*).

Test of Model−Lipid Substitution Experiments. What are the key lipid species that influence the bilayer material properties? The current experiments have explored the relationship between the polymorphic phase properties of DOPE (*81*) and the photochemical activity of rhodopsin. As a specific framework, we have assumed that the curvature stress of the DOPE/DOPC mixtures in the membrane bilayer allows the meta I−meta II change to occur. Two related structural aspects have been examined in detail: (i) the correspondence between formation of nonlamellar phases of the DOPE/DOPC membrane lipid mixtures and the meta I−meta II conformation change and (ii) the mean curvatures of the lipids in the meta II state of the DOPE/DOPC recombinant membranes containing rhodopsin. It is known that DOPE favors the reverse hexagonal H_{II} phase due to its negative spontaneous curvature H_0^L, whereas DOPC favors the lamellar L_α phase, with approximately zero spontaneous curvature (*21*, *81*). The small headgroup size of DOPE relative to the cross-sectional area of the unsaturated oleoyl (18:1) chains yields a curvature elastic stress, due to an imbalance of the lateral forces across the bilayer membrane. By varying the molar ratio of DOPE/DOPC, one has a means of tuning or adjusting the average spontaneous curvature of the membrane. The observation that the meta I/meta II ratio increases progressively with DOPE content implies that curvature stress within the bilayer provides a thermodynamic driving force for the conformational change of rhodopsin (*65*, *66*, *80*).

An important aspect is that we have shown phosphoethanolamine (PE) *headgroups* can substitute for polyunsaturated DHA *chains* in the rhodopsin-containing membrane recombinants. The fact that both PE headgroups and DHA chains have equivalent influences suggests that elastic stress/strain involving the curvature free energy is implicated in modulat-

ing the meta I−meta II transition of rhodopsin (*18*). By approximately doubling the native mole fraction of PE headgroups, essentially the full amount of meta II can be obtained in the DOPE/DOPC recombinant membranes, as in the ROS native membranes. In the native system the PE content is maximal (42%) (*96*), requiring DHA to achieve a sufficiently large curvature free energy (*18*). Analogously, other bulky acyl chains such as phytanic acid can substitute for DHA (*97*). It is interesting that the DOPE/DOPC recombinants as well as the egg PC recombinant and the native ROS membranes all display titration curves which are broadened relative to a simple titration equilibrium. This is to be expected for an amphoteric surface having various acidic or basic functional groups, i.e., due to the presence of rhodopsin. For a titratable surface, the local pH depends on the membrane surface potential ψ_0, leading to a stretching out of the titration curve. Moreover, different meta II species (*64*, *71*, *90*) may be present.

Material Properties of Thin Films—Free Energy Expansion. Here we have treated the continuum thermodynamic properties of membranes in analogy with the nanostructures of surfactant films (*98*) by applying knowledge from colloid and interface science. We consider a generalized expansion of the free energy of a flexible membrane (*99*), involving the following material constants (*13*, *73*): (i) the area elastic modulus k_a and the equilibrium or optimal area per lipid at the aqueous interface A_0^L and (ii) the bending (splay) elastic modulus κ and the spontaneous mean curvature H_0^L of a given monolayer of the bilayer. Alternatively, lattice statistical mechanics (*100*) can be used to derive a microscopic model for the bending elasticity of interfacial surfactant films (*101*) and proteolipid membranes (*62*, *63*, *76*, *102*), or a molecular level theory for lipid−protein interactions can be considered (*6*, *7*). Our approach is to adopt a flexible surface model for coupling the free energy of the membrane lipids to rhodopsin (*3*, *4*), in which the elasticity of the membrane film is linked to alteration of the solvation energy of the protein upon activation. Such a protrusion of rhodopsin from the bilayer may be associated with binding sites for the G protein (transducin) involving the cytoplasmic loops, as indicated by surface plasmon resonance (SPR) spectroscopic measurements (*78*).

Flexible Surface Model in Relation to Free Energy Coupling of Bilayer Lipids to Rhodopsin. According to this new paradigm (*3*, *4*), the free energy coupling involves the elastic stress/strain of the bilayer, together with the local acyl chain packing energy of the lipids. Photolysis of rhodopsin shifts the force balance within the membrane at the meta I state, involving both the lipid/protein interface and the lipid/water interface. An altered Laplace pressure (*4*) acts upon the lipid/protein interface, given by $\Delta P = \gamma_{LP}/r$, where γ_{LP} is the lipid/protein interfacial tension and r is the protein radius (modeled as a cylinder). One possibility is that relief of the lateral stresses in the bilayer (*area frustration*) is linked to the conformational energetics of the membrane-embedded rhodopsin molecules. Alternatively, the meta I−meta II conformational transition may be coupled to a change in the monolayer curvature on either side of the membrane, involving a neutral (dividing) surface where the area is constant (*curvature frustration*) (cf. Figure 1). We have suggested (*4*, *25*) that a natural interpretation involves the curvature free energy of the bilayer associated with the membrane lipid/water interface (*11*, *13*). The curvature strain (displacement) is proportional to $(H^L - H_0^L)$, leading to a curvature stress (force), where the corresponding free energy is given by $\kappa(H^L - H_0^L)^2$. In terms of area strain we obtain that the elastic free energy is given by $k_a(A^L - A_0^L)^2$. In either case, relief of the elastic stress/strain could be linked to a shift of the chain packing energy involving the intramembraneous lipid/rhodopsin surface. One should note that the above considerations pertain exclusively to the intrinsic bilayer part of the free energy (see below). For the case of charged lipids, one needs to separate the contribution from the counterions in the electrical double layer, due to the electrostatic part of the free energy, from the bilayer contributions. However, since the present recombinants involve neutral DOPE/DOPC mixtures, the local pH is close to the bulk pH in the vicinity of the isoelectric point of rhodopsin (cf. Figure 7). Hence, the natural focus is on the *balance* between the bilayer elastic stress/strain and the acyl chain packing (solvation) energy (*4*) and how this balance is affected by lipid−protein interactions in each of the two states of the protein, meta I and meta II.

Lipid Polymorphism and Spontaneous Curvature—Correspondence to Rhodopsin Function? An important aspect involves the correlation between the polymorphic properties of the membrane lipids (*15*, *103*) and the *spontaneous curvature* (H_0^L) of the membrane film (*4*, *11*, *13*). The polymorphism of the amphiphilic molecules is a manifestation of the balance of the attractive and repulsive forces acting at the level of the polar headgroups and nonpolar acyl chains. The spontaneous curvature (or its reciprocal, the spontaneous radius of curvature) explains the formation of nonbilayer lipid structures (*11*−*13*). Simply put, it is the tendency of a given monolayer to curl (*98*, *104*). It is essential to recognize that the spontaneous curvature may or may not correspond to the real or actual curvature of the membrane lipid/water interface. For instance, in the planar L_α phase, with zero mean curvature H^L, the spontaneous curvature may or may not be equal to zero. This is because the additional contribution from the chain stretching also affects the free energy balance. Thus, while each of the opposed monolayers can have a tendency to curve, this is opposed by the chain packing contribution, leading to stabilization of the planar microstructure. In fact, there are two opposite possibilities for the bilayer curvature (*13*, *98*). Typically, amphiphiles with a single chain, such as lysolipids or ordinary detergents, form the normal hexagonal (H_I) phase, which has a positive curvature (toward oil) (*105*). On the other hand, double-chain surfactants such as phospholipids adopt the reverse hexagonal (H_{II}) phase, with a negative curvature (toward water) (*14*).

What is the correspondence to the photochemical activity of rhodopsin? Here PC can be considered as a reference system, which together with saturated or monounsaturated acyl chains yields a small or zero spontaneous curvature, so that the planar L_α phase of the bilayer and hence meta I are favored (*4*, *25*). Investigations have revealed that lipids giving rise to a nativelike photochemical function of rhodopsin have a tendency to form nonlamellar phases in the absence of protein. The presence of only PC together with DHA does not suffice to yield full meta II formation (*18*). Recombinants with PE alone favor formation of meta II (*18*) but again do

not give maximum photochemical activity (*3*, *18*), and recombinants with PS behave similarly (*84*). In this regard, it is known that phospholipids having PE headgroups together with DHA tend to adopt the nonlamellar, reverse hexagonal (H_{II}) phase (*10*). The native mixture of headgroups comprising PC, PE, and PS together with polyunsaturated DHA chains is close to a $L_\alpha - H_{II}$ phase boundary (*10*, *94*) and is sufficient for maximum photochemical function of rhodopsin (*18*). The combination of relatively small PE headgroups together with bulky, polyunsaturated (DHA) chains leads to a large negative spontaneous curvature. The negative spontaneous curvature of the lipids (toward water) favors the activated meta II form by relief of the curvature frustration of the bilayer lipids (*4*, *25*). Moreover, the PE polar headgroups are able to compensate for the contribution to H_0 from the polyunsaturated DHA chains, as noted above. By contrast, PS favors meta II due to its influence on the concentration of hydronium ions, H_3O^+, in the electrical double layer, which favor proton uptake by rhodopsin and formation of the meta II product (*84*, *93*). Yet this is opposed by the effect of PS on the bilayer lipid spontaneous curvature, which stabilizes the planar L_α state and, thus, the reactant meta I. These opposite or paradoxical influences of PS render the membrane sensitive to the surface charge density in the physiological pH range (*83*, *84*) and thus to phosphorylation of rhodopsin (*72*).

Matching of Lipid Spontaneous Curvature to the Lipid/Protein Interface. In the current work, we have investigated this functional agonism or antagonism involving the lipid polar headgroups and the acyl chains in further detail. We specifically tested whether matching of the average spontaneous curvature H_0^L of the lipids to the bilayer curvature H^L adjacent to the lipid/protein interface can be the determinant of protein conformation and function (*3*, *4*, *18*). For the pure lipid systems, increasing the amount of DOPE relative to DOPC leads to formation of the H_{II} phase, where a smaller radius of curvature corresponds to a larger (negative) monolayer spontaneous curvature (H_0) (*81*). The present work reveals that matching of the spontaneous curvature (*3*, *4*) of the DOPE/DOPC mixtures can explain the effects of the bilayer lipid composition in the case of rhodopsin. We propose that *lipid agonists* for the activation of rhodopsin, in a strict operational sense, act by increasing the elastic stress/strain in the meta I state and/or decreasing the chain packing energy (protein solvation energy) in the meta II state. In the case of rhodopsin lipid agonists have a *negative spontaneous curvature*. Consequently, there is a shifting of the equilibrium to the right, toward the activated meta II state. By contrast, *lipid antagonists* act oppositely, again in a strictly operational sense. For rhodopsin the lipid antagonists have approximately *zero spontaneous curvature* and yield an increased elastic stress/strain in the meta II state, possibly together with an increase in chain packing energy. Hence the meta I−meta II equilibrium is shifted to the left, toward the inactive meta I state. The above formulation leads to the new principle of matching the spontaneous curvature of the bilayer lipids to the mean curvature of the lipid/water interface adjacent to the protein as a unifying biophysical paradigm.

New Biomembrane Model. The influences of lipid polymorphism and the role of the (average) spontaneous curvature

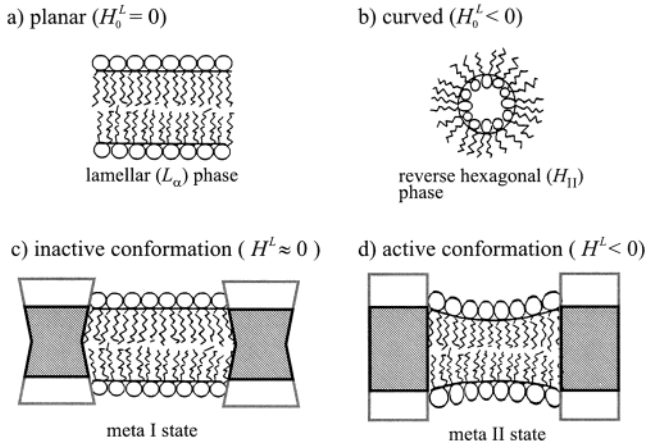

FIGURE 9: Schematic illustration of the flexible surface model for coupling the free energy of bilayer lipids to the conformational energetics of an integral membrane protein. (a) Planar, liquid-crystalline (L_α) phase of lipids having zero spontaneous curvature, H_0^L. (b) Cross section through a reverse hexagonal (H_{II}) phase lipid nanotube, with a negative spontaneous curvature. (c) Inactive conformation of a membrane protein stabilized by lipids with approximately zero spontaneous curvature. (d) Cross section through the active conformational state involving nonlamellar-forming lipids with negative spontaneous curvature. Matching of the *spontaneous curvature* of the membrane lipids to the curvature at the lipid/protein interface H^L gives a means of coupling the free energies of the two components (cf. text).

of the membrane lipid bilayer (*4*, *25*) are summarized schematically in Figure 9. We propose that phospholipids such as DOPC which have approximately zero spontaneous curvature H_0^L favor the planar (L_α) state, part a, and stabilize the meta I form of rhodopsin. Conversely, phospholipids such as DOPE with a negative spontaneous curvature H_0^L (toward water) form the reverse hexagonal (H_{II}) (or inverted cubic) phase, part b, and stabilize the meta II conformation. Part c of Figure 9 shows the inactive meta I state of the membrane, where the mean curvature H^L of the bilayer lipids is approximately zero, thus matching H_0^L of the L_α-forming lipids; cf. part a. Last, part d indicates the activated meta II state in cross section, in which rhodopsin is more exposed (*78*) and the membrane surface has a negative mean curvature H^L, geometrically conforming to H_0^L of the H_{II}-forming lipids in part b. Due to the meta I−meta II conformational change of rhodopsin, the curvature frustration of the membrane is reduced in the meta II state, which balances the energetic cost of the increased intramembraneous hydrophobic protein surface. It follows that the curvature free energy change of the membrane in the meta I−meta II equilibrium is energetically coupled to the mechanical work of rhodopsin photoexcitation in the visual process. From the slope of the curve in Figure 8, part a, one can estimate the difference in average curvatures of the lipids in the meta I and meta II states. An heuristic calculation assumes $\kappa \approx 10\ k_BT$ and $N = 50$ (per monolayer), with $A = 70$ Å^2/lipid, $H_0^{DOPE} = 1/40$ Å, and $R_{MI} = 2R_{MII}$. Applying eq 17, we estimate $R_{MII} \approx 350$ Å for the curvature radius in the meta II state, consistent with a balance of the curvature free energy and the protein solvation energy (vide supra). The corresponding value of ΔG_c, using eq 16b, is -4.8 kJ mol^{-1} for $X_{DOPE} = 0.75$ at pH 7.0. Thus, a more negative curvature at the lipid/protein interface in the meta II state versus meta I would provide a means of free energy coupling of the

bilayer lipids to rhodopsin. Exposure of the G protein binding sites of rhodopsin can thus be controlled by properties of the membrane lipid bilayer.

In consequence, the meta I state of rhodopsin is energetically favored by lipids forming the L_α phase, whereas the meta II state is stabilized by lipids tending to form the nonlamellar H_{II} or cubic phases. Moreover, for recombinant bilayers containing cholesterol, we suggest a *decrease* in H_0^L favors the planar L_α state (*4*) and hence formation of meta I as observed experimentally (*33*, *60*). By contrast, osmotic stress increases the magnitude of H_0^L due to a dehydration of the lipids (*13*) and favors meta II, in agreement with experimental observations (*34*). In this manner, we are able to account for the influences of diverse membrane lipids on the conformational energetics of photolyzed rhodopsin associated with visual signal transduction. A role of nonspecific biophysical properties of the lipid bilayer is suggested, centering about the nonlamellar forming tendency of the mixtures in relation to the photochemical function of rhodopsin, as defined by the meta I−meta II transition. It is both the strength and weakness of our approach that molecularly specific details are not explicitly considered. Accordingly, the dependence of the meta I−meta II equilibrium of rhodopsin on the lipid curvature energy reinforces the hypothesis that rhodopsin functions optimally when the membrane is under curvature elastic stress (*18*).

BIOCHEMICAL CONCLUSIONS

The issues of lipid diversity and lipid regulation of cellular function are addressed in this paper within the framework of a new biomembrane model. Typically, in biochemistry textbooks only the planar, lamellar phase of the membrane lipids is described, as in the standard fluid-mosaic model of biomembrane structure. Yet evidence is increasing that the presence of lipids with a tendency to form nonlamellar phases close to the physiological conditions plays a significant role in membrane-related activities. Deformation of the bilayer in conjunction with protein conformational changes explains the lipid influences on key membrane functions, such as visual signal transduction. Here we have further tested a new flexible surface model (*4*) involving a nonspecific mechanism for coupling the free energy of the bilayer lipids to membrane proteins. The central idea involves extending the concept of the monolayer curvature free energy, as formulated by Helfrich (*59*) for surfactant films, to the mesoscopic length scale characteristic of lipid−protein interactions. In a phospholipid membrane, there can be an appreciable bending energy associated with instability of the bilayer. This renders the meta I−meta II transition of rhodopsin sensitive to the spontaneous curvature of the membrane lipids. The above hypothesis predicts that the lowest energy state of the membrane is one in which the curvature free energy of the lipid film is balanced by the solvation energy of the lipid/protein interface. This new principle involves matching the *spontaneous curvature* of the lipids to the local curvature of the bilayer surface adjacent to the protein as a unifying paradigm. Biological activity can then be regulated by membrane lipids whose spontaneous curvature most closely matches the active state of the proteolipid assembly. The compensatory influences of the polar headgroups and acyl chains of membrane lipids point to the role of chemically nonspecific material properties of the membrane bilayer in governing the conformational energetics of membrane proteins, e.g., G protein-coupled receptors such as rhodopsin. Thus the tightly regulated composition of the retinal rod membranes may involve mixtures of nonlamellar-forming lipids having material properties which govern the conformational energetics of rhodopsin in the process of visual signal transduction.

ACKNOWLEDGMENT

We are grateful to Gary Martinez for computing assistance and Thomas Huber for many valuable discussions during the course of this work. Thanks are also due to John Rupley, Gordon Tollin, and the referees for helpful criticisms of the manuscript.

REFERENCES

1. Singer, S. J., and Nicolson, G. L. (1972) *Science 175*, 720−731.
2. Gennis, R. B. (1989) *Biomembranes. Molecular Structure and Function*, Springer-Verlag, New York.
3. Gibson, N. J., and Brown, M. F. (1993) *Biochemistry 32*, 2438−2454.
4. Brown, M. F. (1994) *Chem. Phys. Lipids 73*, 159−180.
5. Nielsen, C., Goulian, M., and Andersen, O. S. (1998) *Biophys. J. 74*, 1966−1983.
6. May, S., and Ben-Shaul, A. (1999) *Biophys. J. 76*, 751−767.
7. Nielsen, C., and Andersen, O. S. (2000) *Biophys. J. 79*, 2583−2604.
8. Brown, M. F., Thurmond, R. L., Dodd, S. W., Otten, D., and Beyer, K. (2001) *Phys. Rev. E 64*, 010901-1−010901-4.
9. Cullis, P. R., and de Kruijff, B. (1979) *Biochim. Biophys. Acta 559*, 399−420.
10. Brown, M. F., Deese, A. J., and Dratz, E. A. (1982) *Methods Enzymol. 81*, 709−728.
11. Gruner, S. M. (1989) *J. Phys. Chem. 93*, 7562−7570.
12. Lindblom, G., and Rilfors, L. (1989) *Biochim. Biophys. Acta 988*, 221−256.
13. Seddon, J. M. (1990) *Biochim. Biophys. Acta 1031*, 1−69.
14. Thurmond, R. L., Lindblom, G., and Brown, M. F. (1993) *Biochemistry 32*, 5394−5410.
15. de Kruijff, B. (1997) *Curr. Opin. Chem. Biol. 1*, 564−569.
16. Navarro, J., Toivio-Kinnucan, M., and Racker, E. (1984) *Biochemistry 23*, 130−135.
17. Jensen, J. W., and Schutzbach, J. S. (1988) *Biochemistry 27*, 6315−6320.
18. Wiedmann, T. S., Pates, R. D., Beach, J. M., Salmon, A., and Brown, M. F. (1988) *Biochemistry 27*, 6469−6474.
19. Epand, R. M. (1990) *Biochem. Cell Biol. 68*, 17−23.
20. Killian, J. A., van den Berg, C. W., Tournois, H., Keur, S., Slotboom, A. J., van Scharrenburg, G. J. M., and de Kruijff, B. (1986) *Biochim. Biophys. Acta 857*, 13−27.
21. Keller, S. L., Bezrukov, S. M., Gruner, S. M., Tate, M. W., Vodyanoy, I., and Parsegian, V. A. (1993) *Biophys. J. 65*, 23−27.
22. Epand, R. M. (1998) *Biochim. Biophys. Acta 1376*, 353−368.
23. Lundbaek, J. A., and Andersen, O. S. (1999) *Biophys. J. 76*, 889−895.
24. Lewis, J. R., and Cafiso, D. S. (1999) *Biochemistry 38*, 5932−5938.
25. Brown, M. F. (1997) *Curr. Top. Membr. 44*, 285−356.
26. Teller, D. C., Okada, T., Behnke, C. A., Palczewski, K., and Stenkamp, R. E. (2001) *Biochemistry 40*, 7761−7772.
27. Farrens, D. L., Altenbach, C., Yang, K., Hubbell, W. L., and Khorana, H. G. (1996) *Science 274*, 768−770.
28. Altenbach, C., Cai, K. W., Khorana, H. G., and Hubbell, W. L. (1999) *Biochemistry 38*, 7931−7937.
29. Hubbell, W. L., Cafiso, D. S., and Altenbach, C. (2000) *Nat. Struct. Biol. 7*, 735−739.

30. Palczewski, K., Kumasaka, T., Hori, T., Behnke, C. A., Motoshima, H., Fox, B. A., Le Trong, I., Teller, D. C., Okada, T., Stenkamp, R. E., Yamamoto, M., and Miyano, M. (2000) *Science 289*, 739−745.
31. Beach, J. M., Pates, R. D., Ellena, J. F., and Brown, M. F. (1984) *Biophys. J. 45*, 292a.
32. Baldwin, P. A., and Hubbell, W. L. (1985) *Biochemistry 24*, 2624−2632.
33. Mitchell, D. C., Straume, M., and Litman, B. J. (1992) *Biochemistry 31*, 662−670.
34. Mitchell, D. C., and Litman, B. J. (1999) *Biochemistry 38*, 7617−7623.
35. Mitchell, D. C., and Litman, B. J. (2000) *J. Biol. Chem. 275*, 5355−5360.
36. Niu, S. L., Mitchell, D. C., and Litman, B. J. (2001) *J. Biol. Chem. 276*, 42807−42811.
37. Mitchell, D. C., Niu, S. L., and Litman, B. J. (2001) *J. Biol. Chem. 276*, 42801−42806.
38. Khorana, H. G. (1993) *Proc. Natl. Acad. Sci. U.S.A. 90*, 1166−1171.
39. Sakmar, T. P., and Fahmy, K. (1995) *Isr. J. Chem. 35*, 325−337.
40. Kliger, D. S., and Lewis, J. W. (1995) *Isr. J. Chem. 35*, 289−307.
41. Lee, A. G. (1998) *Biochim. Biophys. Acta 1376*, 381−390.
42. Rankin, S. E., Addona, G. H., Kloczewiak, M. A., Bugge, B., and Miller, K. W. (1997) *Biophys. J. 73*, 2446−2455.
43. Chang, H. M., Reitstetter, R., Mason, R. P., and Gruener, R. (1995) *J. Membr. Biol. 143*, 51−63.
44. Lindblom, G., Brentel, I., Sjölund, M., Wikander, G., and Wieslander, Å. (1986) *Biochemistry 25*, 7502−7510.
45. Dowhan, W. (1997) *Annu. Rev. Biochem. 66*, 199−232.
46. Kinnunen, P. (1996) *Chem. Phys. Lipids 81*, 151−166.
47. Harroun, T. A., Heller, W. T., Weiss, T. M., Yang, L., and Huang, H. W. (1999) *Biophys. J. 76*, 937−945.
48. Andersen, O. S., Apell, H. J., Bamberg, E., Busath, D. D., Koeppe, R. E., Sigworth, F. J., Szabo, G., Urry, D. W., and Woolley, A. (1999) *Nat. Struct. Biol. 6*, 606−609.
49. Miljanich, G. P., Nemes, P. P., White, D. L., and Dratz, E. A. (1981) *J. Membr. Biol. 60*, 249−255.
50. Dratz, E. A., and Deese, A. J. (1986) in *Health Effects of Polyunsaturated Fatty Acids in Seafoods* (Simopoulos, A. P., Kifer, R. R., and Martin, R. E., Eds.) pp 379−412, Academic Press, New York.
51. Anderson, R. E., Maude, M. B., Narfström, K., and Nilsson, S. E. G. (1997) *Exp. Eye Res. 64*, 181−187.
52. Bush, R. A., Malnoe, A., Reme, C. E., and Williams, T. P. (1994) *Invest. Ophthalmol. Vis. Sci. 35*, 91−100.
53. Isele, J., Sakmar, T. P., and Siebert, F. (2000) *Biophys. J. 79*, 3063−3071.
54. Hessel, E., Müller, P., Herrmann, A., and Hofmann, K. P. (2001) *J. Biol. Chem. 276*, 2538−2543.
55. Mouritsen, O. G., and Bloom, M. (1984) *Biophys. J. 46*, 141−153.
56. Bloom, M., Evans, E., and Mouritsen, O. G. (1991) *Q. Rev. Biophys. 24*, 293−397.
57. London, E., and Brown, D. A. (2000) *Biochim. Biophys. Acta 1508*, 182−195.
58. Miljanich, G. P., Brown, M. F., Mabrey-Gaud, S., Dratz, E. A., and Sturtevant, J. M. (1985) *J. Membr. Biol. 85*, 79−86.
59. Helfrich, W. (1973) *Z. Naturforsch. 28*, 693−703.
60. Mitchell, D. C., Straume, M., Miller, J. L., and Litman, B. J. (1990) *Biochemistry 29*, 9143−9149.
61. Cantor, R. S. (1997) *J. Phys. Chem. B 101*, 1723−1725.
62. Cantor, R. S. (1997) *Biochemistry 36*, 2339−2344.
63. Cantor, R. S. (1999) *Biophys. J. 76*, 2625−2639.
64. Hofmann, K. P., Jäger, S., and Ernst, O. P. (1995) *Isr. J. Chem. 35*, 339−355.
65. Gibson, N. J., and Brown, M. F. (1993) *Biophys. J. 64*, A20.
66. Brown, M. F., Gibson, N. J., and Thurmond, R. L. (1996) *Biophys. J. 70*, A422.
67. Papermaster, D. S., and Dreyer, W. J. (1974) *Biochemistry 13*, 2438−2444.
68. Hong, K., and Hubbell, W. L. (1973) *Biochemistry 12*, 4517−4523.
69. Wang, Y. (1997) Ph.D. Dissertation, University of Arizona.
70. Parkes, J. H., and Liebman, P. A. (1984) *Biochemistry 23*, 5054−5061.
71. Arnis, S., and Hofmann, K. P. (1993) *Proc. Natl. Acad. Sci. U.S.A. 90*, 7849−7853.
72. Gibson, S. K., Parkes, J. H., and Liebman, P. A. (1999) *Biochemistry 38*, 11103−11114.
73. Israelachvili, J. N. (1992) *Intermolecular and Surface Forces*, 2nd ed., Academic Press, San Diego.
74. Petrache, H. I., Dodd, S. W., and Brown, M. F. (2000) *Biophys. J. 79*, 3172−3192.
75. Anderson, D. M., Gruner, S. M., and Leibler, S. (1988) *Proc. Natl. Acad. Sci. U.S.A. 85*, 5364−5368.
76. Cantor, R. S. (1999) *Chem. Phys. Lipids 101*, 45−56.
77. Altenbach, C., Cai, K. W., Klein-Seetharaman, J., Khorana, H. G., and Hubbell, W. L. (2001) *Biochemistry 40*, 15483−15492.
78. Salamon, Z., Brown, M. F., and Tollin, G. (1999) *Trends Biochem. Sci. 24*, 213−219.
79. Mitchell, D. C., and Litman, B. J. (1994) *Biochemistry 33*, 12752−12756.
80. Botelho, A. V., Gibson, N. J., Wang, Y., Thurmond, R. L., and Brown, M. F. (2001) *Biophys. J. 80*, 547a.
81. Rand, R. P., Fuller, N. L., Gruner, S. M., and Parsegian, V. A. (1990) *Biochemistry 29*, 76−87.
82. McLaughlin, S. (1989) *Annu. Rev. Biophys. Biophys. Chem. 18*, 113−136.
83. Hubbell, W. L. (1990) *Biophys. J. 57*, 99−108.
84. Gibson, N. J., and Brown, M. F. (1991) *Biochem. Biophys. Res. Commun. 176*, 915−921.
85. Tsui, F. C., Ojcius, D. M., and Hubbell, W. L. (1986) *Biophys. J. 49*, 459−468.
86. Tsiu, F. C., Sundberg, S. A., and Hubbell, W. L. (1990) *Biophys. J. 57*, 85−97.
87. Stone, W. L., Farnsworth, C. C., and Dratz, E. A. (1979) *Exp. Eye Res. 28*, 387−397.
88. Falk, G., and Fatt, P. (1968) *J. Physiol. 198*, 647.
89. Fung, B. K., Hurley, J. B., and Stryer, L. (1981) *Proc. Natl. Acad. Sci. U.S.A. 78*, 152−156.
90. Okada, T., Ernst, O. P., Palczewski, K., and Hofmann, K. P. (2001) *Trends Biochem. Sci. 26*, 318−324.
91. Fung, B. K., and Hubbell, W. L. (1978) *Biochemistry 17*, 4403−4410.
92. Nathans, J. (1990) *Biochemistry 29*, 937−942.
93. Gibson, N. J., and Brown, M. F. (1991) *Photochem. Photobiol. 54*, 985−992.
94. Deese, A. J., Dratz, E. A., and Brown, M. F. (1981) *FEBS Lett. 124*, 93−99.
95. Gruner, S. M. (1985) *Proc. Natl. Acad. Sci. U.S.A. 82*, 3665−3669.
96. Miljanich, G. P., Sklar, L. A., White, D. L., and Dratz, E. A. (1979) *Biochim. Biophys. Acta 552*, 294−306.
97. Brown, M. F., and Gibson, N. J. (1992) in *Essential Fatty Acids and Eicosanoids* (Sinclair, A., and Gibson, R., Eds.) pp 134−138, American Oil Chemists' Society Press, Champaign, IL.
98. Olsson, U., and Wennerström, H. (1994) *Adv. Colloid Interface Sci. 49*, 113−146.
99. Evans, D. F., and Wennerström, H. (1999) *The Colloidal Domain*, Wiley-VCH, New York.
100. Dill, K. A., Naghizadeh, J., and Marqusee, J. A. (1988) *Annu. Rev. Phys. Chem. 39*, 425−461.
101. Cantor, R. S. (1993) *J. Chem. Phys. 99*, 7124−7149.
102. Cantor, R. S. (1999) *Biophys. J. 77*, 2643−2647.
103. Cullis, P. R., and de Kruijff, B. (1978) *Biochim. Biophys. Acta 513*, 31−42.
104. Anderson, D. M., and Wennerström, H. (1990) *J. Phys. Chem. 94*, 8683−8694.
105. Thurmond, R. L., Otten, D., Brown, M. F., and Beyer, K. (1994) *J. Phys. Chem. 98*, 972−983.

BI011995G